

# A REVIEW OF FRICTION WELDING RESEARCH ADDRESSING THE INFLUENCE, DEVELOPMENT, SIMILAR & DISSIMILAR WELDING

S. Senthil Murugan<sup>1\*</sup>, P. Sathiya<sup>2</sup>

<sup>1</sup>Rajalakshmi Engineering College (Autonomous), Chennai - 602105, Tamilnadu, India

<sup>2</sup>National Institute of Technology, Tiruchirappalli - 620015, Tamilnadu, India

\*Corresponding author's email: gctsegan@gmail.com

## ABSTRACT

*This review paper discusses the recent research work carried out in the frictional joining of dissimilar and similar alloys through the friction welding (FW) process with various parameters and modifications. It includes further the latest developments and advances in the research on FW and the influences of FW's process parameters on the quality of joints and their properties. The specimens' faying surfaces can also influence the joint properties as the surface modifications stimulate or change the metal joints' bonding according to the welding parameters selected during FW. Though the rise of friction pressure (FP) during FW improves the strength of the joints, the improper selection of parameters leads to metal damage. It feels better if the axial shortening is less than 30 mm for FW of soft metals. The axial shortening values are less than 25 mm for the hemispherical bowl-type faying surfaces under 18 bar FP and it is noted that the bevel-type tapered faying surfaces increase the shortening. FW provided very narrow weld interfaces with around 5-10  $\mu\text{m}$  width. With a low FP, it was possible to obtain a maximum of 100 % efficiency by modifying their faying surfaces. The small-diameter soft material needs less FP and friction time. The microstructure modification is possible and the weld joint is shown as U and V shapes for the bowl and tapered faying surfaces. It further increases the contact area and thus increases strength.*

**KEYWORDS:** faying surfaces, friction welding, dissimilar alloys, mechanical, heat affected zone

## 1. INTRODUCTION

The frictional joining of metals is successfully possible due to the frictional effect generated by the rotary action and it is more admired owing to its benefits, for instance, ease of controlling the parameters, less metal wastage, less fabrication time required and high production rate, the possibility of dissimilar metal joining, and admirable weld performance [1]. The significant issues to be considered during FW comprise the development of brittle intermetallic in the weld interface (WI), the width of the heat-affected zone (HAZ) and the interface temperature [2]. However, FW has the worth of producing sound joints (dissimilar/similar) with narrow HAZ, thermo-mechanically affected zone (TMAZ) and minor intermetallic at low interface temperature. In rotary friction welding (RFW) (Fig. 1), the coalescence is attained by the synergic effects of a relative motion between the parts to be welded and the pressure.

In FW, both temperatures generated and the stresses developed govern the welding parameters, so

knowledge is necessary to recognize the optimum parameters for improving the design of joining dissimilar materials. The works related to faying surface modifications on dissimilar weld specimens were not widely found in the literature. It is tricky to join ferrous austenitic stainless steel 304 and 316 alloys with non-ferrous aluminium 6000 series dissimilar metals using conventional fusion welding techniques since they have different properties and compositions. It forms brittle intermetallic compounds at the weld interface (WI) at high temperatures. As a result, joining such dissimilar alloys is a challenging task with maximum joining efficiency.

No research was found on FW with surface modifications like buttering or dip coating, tapering and deep recess combinations, tapering, interlayer with Cr, threaded surfaces, and hemispherical for AA6063 & AISI304L. These research gaps are fulfilled by this investigation.

Various combinations of dissimilar materials, joined by FW, was witnessed through the literature survey, and presented in Table 1.

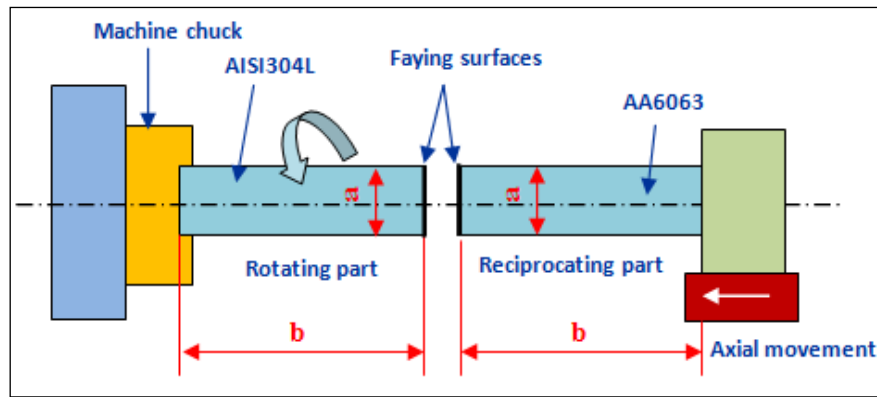


Fig. 1. Graphic image of rotary friction welding set-up (a - rod diameter, b - length of samples to be welded)

Table 1. Combinations of Dissimilar metals joining research through FW

Combinations of dissimilar metals for the research	Authors and year
Ferritic Stainless Steel and Austenitic Stainless Steel	Manideep D. and Balachandar K. 2012 [1]
Aluminium and brass	Wang G L et al. [2]
316L Austenitic Stainless Steel and 1045 Medium Carbon Steel	Gawhar Ibraheem Khidhir, and Sherko.A. Baban 2019 [3]
AA2024 alloy and SS304 steel	Chennakesava R. Alavala 2016 [4]
AA5052 alloy and AISI 304	Honggang Dong et al. 2020 [5]
AA6061 and AISI304	Madhusudhan G. Reddy et al. 2008 [6]
AISI4340 and AA6061 -T6	Suresh D. Meshram and Madhusudhan Reddy G. 2015 [7]
AA6061-T6 matrix composite and AISI304	Kannan P et al. 2015 [8]
AA6063 and AISI304L	Senthil et al. 2020 [9]
AA6082 and Ti-6Al-4V	Meisnar M et al. 2017 [10]
AISI1018 steel and AA6061-T6 alloy	Emel Taban et al. 2010 [11]
AISI1020 and ASTM A536	Radosław Winiczenko 2016 [12]
AISI304 and AA6063	Kimura M et al. 2006 [13]
AISI304L and AISI1040	Jeswin Alphy James, and Sudhish R 2016 [14]
AISI304L and P91 alloy steel	Javed Akram et al. 2017 [15]
Alumina-Mullite Composite and AA6061	Marjan Safarzadeh et al. 2016 [16]
SAE1020 Steel and Aluminum 6351- T6	Marlon A. Pinheiro and Alexandre Q. Bracarense 2019 [17]
Brass and High Carbon Steel	Jian Luo et al. 2012 [18]
C44300 copper alloy and AA7075-T651 alloy	Radhakrishnan. E et al. 2019 [19]
Carbon Steel to Stainless	Hong Ma et al. 2015 [20]
Stainless steel and aluminium	Mumin Sahin 2009 [21]
copper and aluminium	Mumin Sahin 2010 [22]
Copper and Aluminium	Longwei Pan et al. 2018 [23]
Mild Steel and Al6061 and Alumina	Hazman Seli et al. 2013 [24]
Mild Steel and Aluminium	Hazman Seli et al. 2010 [25]
mild steel and titanium	Prasanthi T. N. et al. 2015 [26]
P91 and Nickel	Akram J et al. 2018 [27]
Pure aluminium and SS304	Kimura M et al. 2017 [28]
Pure magnesium and pure aluminium	Kimura M et al. 2015 [29]
Ni-based superalloy and heat-resistant steel	Kimura M et al. 2019 [30]
Ti-6Al-4V and SS304L	Kumar R and Balasubramanian M 2015 [31]
Tini Alloy to Stainless Steel	Fukumoto S et al. 2010 [32]
Titanium and AISI304	Muralimohan CH et al. 2016 [33]
TZM Mo-base powder alloy and H11 mould steel	Fu Li and Du Suigeng 2001 [34]

## 2. DEVELOPMENTS IN FW RESEARCH

The researchers claimed that the finite element method (FEM) and Python can also be used to model a joint with high quality and predict the microstructure and temperature distribution [35, 36]. The grain refinement is also possible by the frictional joining; it was proved that the grain construction and the recrystallization are the main microstructure modifications due to the FW [37]. A victorious weld between the dissimilar materials is as strong as the soft materials of the two being joined. The research informed us that the quality of the weld obtained can be checked and the crack can be found with the help of the image segmentation technique as the coefficient of friction (COF) between the metals during FW is major [38]. The complexity of joining dissimilar metals depends on the excellence of the transition zone in the joint and the intermetallic phases that take place in this transition zone. For this case, a discontinuous layer structured during the FW between pure Al/ Fe at the joint interface created the failure almost at the joints [39]. Dissimilar welding is successful only if there is mutual solubility of the two metals [40]. But if there is no solubility or little between the two different metals that are to be joined, the weld joint will not be successful. Otherwise, it is necessary to use a third metal as an interlayer that is soluble with each metal to fabricate a successful joint. The transition zone (TZ) has to be studied to find out its crack sensitivity, strength and susceptibility to corrosion [41]. If the coefficient of thermal expansion (CTE) of both materials is extensively unlike, then there would be internal stresses set up in the intermetallic zone during any temperature change of the weldment. Thermal expansion plays a vital role in the failures of the dissimilar weld by developing high stress at the weld interface [27]. If the intermetallic zone is brittle it may lead to weld failure soon. The dissimilarity in the melting point of dissimilar metals to be joined must be considered since one metal will be in the molten stage long before the other when subjected to the same heat amount.

According to Daniel Soares de Alcantara et al. [42], the FW process is an experimentally proved concept. The friction between the faying surfaces can alter the deformation depending on the weld material viscosity during the welding. The vibration signals caused by the dynamic behaviour of the FW machine such as speed, forging axial pressures etc. can be converted into other required information. Long duration in welding (friction time) and high rotational speed in rpm produce lower vibration amplitude. It was recorded that the high vibration energy is generated during the frictional joining stage in the FW and produces changes in the thermo-mechanical couples. The amplitude of vibration is higher at the centre rather than in the outer region during the joining process. According to Wei Zou and Werner Karl Schomburg [43], there was a development in the FW machine with a sensor of piezoelectric and pyroelectric polymer polyvinylidene fluoride. The significance of this sensor arrangement is to measure the temperature developed during the friction between the faying surfaces of the weld specimens and to measure the shear stress formed during the process. Apart from this, other advantages are monitoring the duration of starting and stopping the process, dynamic activity, heating and cooling rate monitoring etc. The time-measuring accuracy was about 100 kHz. With the help of this advancement, the optimum pressure can be obtained for the process. A new method was developed in friction welding (inertia) to address the efficiency with a torque load cell attached to the non-rotating workpiece, while the rotating part is determined by the deceleration rate of the flywheel. Another new technique called friction crush welding (FCW) offers versatile applications in welding sheet metals [44]. Koen Faes and his team of Denys NV developed a new FW technique called FRIEX (Figure 2.a-c [45]), a new friction welding method for joining similar/dissimilar pipes in various sizes. As the pipes are too long, it is difficult to weld using conventional FW, so the FRIEX was implemented.

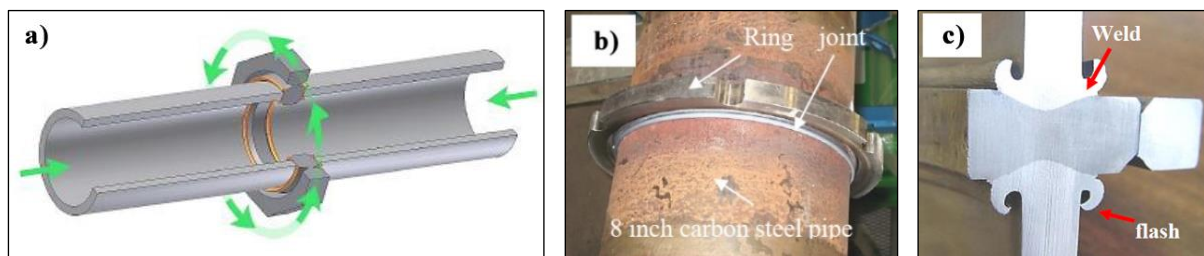


Fig. 2. FRIEX process: a) principle; b) pipe welding; c) macrostructure [45]

## 3. FW OF SIMILAR METALS

Koshiro Aoki and Takuyu Koezawa [46] studied the effect of the FW technique in joining equal channel angular extrusion (ECAE) deformed 6063-T5 aluminium alloy, and reported that the ECAE process

improves the welding efficiency by above 70%. Iracheta. O et al. [47] used inertia FW (IFW) to weld CrMoV-based steel and developed a finite element model to predict the residual stress during the IFW. The authors did some research on welding TC-17 titanium alloy by linear FW (LFW) and measured the internal

residual stress distribution using the contour method. Gianluca Buffa et al. [48] used the LFW process for joining the aluminium 2011-T3 alloy to identify the temperature-dependent friction coefficient and shear stress acting on the weld zone. This research is used to understand the bonding mechanism of the LFW process. Supriya Nandy et al. [49] researched AA6063 alloy to predict yield strength through the classical model and Orowan model. Their research concluded that the Orowan model is better to predict the yield strength and the results are useful to develop maps for thermal processing to attain a needed level of yield strength for AA6063 alloy for the joining. Gianluca Buffa et al. [50] developed a numerical integrated tool for forecasting the weld quality in joining AA6082 aluminium alloy through the FW process. The effectiveness of the tool was explained in their research. Prashanth. K.G et al. [51] did FW of Al-12Si metal generated by selective laser melting process. The results showed an improvement in ductility whereas the drop in hardness in the weld interface compared to the base metal.

Feng Jin et al. [52] experimented on the DDFW of SUS304 in the diameter of  $\phi 25$  mm at 80 MPa. A 2D FEA model was constructed to simulate the thermo-mechanical coupling during welding. The results show that the corona-bond develops and fills out the interface, in which the temperature is rising. According to the research of Peng Li et al. [53], the sound weld joint of AlCoCrFeNi<sub>2.1</sub> eutectic high entropy alloy (EHEA) is possible by rotary FW (RFW). Mohammed Asif. M. et al. [54] did research on the effect of heat in the preparation of UNS S31803 duplex stainless steel using the FW process. They found that the grain refinement was possible by the increase in heat and thus it increases the microhardness near the weld interface. The corrosion resistance was much better in the weld zone than that of base metal with the increase of heat during FW. The research also suggested the frictional joining of the plastically deformed materials using metal forming processes like equal channel angular process, equal channel angular extrusion, etc., such kind of research was done by Mumin Sahin et al. [55]. They joined the aluminium 5083 alloy that was severely deformed for one pass by the equal channel angular pressing method. They found that the mechanical properties were improved due to the deformation process in addition to refining the grains. It was known that if the pass level in the equal channel process was increased as one-pass, two-pass etc., then the joining yielded higher hardness and strength.

Raab. U et al. [56] did research on the joining of titanium (Ti) alloy through both orbital and linear FW processes with identical weld parameters and their results were compared. The results showed that orbital FW needed a shorter time for the weld preparation compared to linear FW and the heat generation was also more due to the orbital speed. The continuous orbital speed improved much stronger than that of the reciprocating speed in the linear FW process.

Radoslaw Winiczenko and Mieczyslaw Kaczorowski [57] studied the FW of ductile cast iron with pure Armco iron, stainless steel, and low-carbon steel interlayers. Though the diffusion took place in a short duration, the amount of diffusion was huge enough with good plastic deformation. Chromium carbide due to the carbon atom was formed in the grain boundaries. The interface of stainless-steel interlayer and ductile cast iron had the transmission of chromium and nickel elements across its boundary.

Mumin Sahin [58] proved the FW of plastically deformed austenitic stainless steel alloys and studied the microstructure, hardness and tensile strength of the joint. The author tried welding the alloy at different diameter ratios. The tensile strength of the joint decreased since the diameter ratio increased. The results showed that the weld specimens having equal diameters had maximum strength equal to 795 MPa at 60 MPa friction pressure and 9 sec. Friction time. The improvement in grains due to the frictional effect could be seen in the microstructures of weld regions, but the plastic deformation of stainless steel alloy used in this study showed no effect on the hardness values and the FW parameters. Ma. T.J. et al. [59] did linear FW of the nickel-based superalloy at the friction force of 16 tons. Microstructures showed the fine grain structures in weld zones. Thermo-mechanically affected zones (TMAZ) showed no deformation. It was reported that Fe<sub>2</sub>Al<sub>5</sub> intermetallic was confirmed along the grain boundaries, which reduced the joint property. The Tensile and Vickers hardness of the joint were low compared to the base metal. The research disclosed that the long duration of friction time was showing unsatisfactory results. Tiejun Ma et al. [60] studied the performance of the joint of single-crystal nickel-based alloy fabricated through the linear FW process. A polycrystalline microstructure was formed in the weld zone due to the thermal and mechanical effects during the welding. The results showed that the hardness and tensile values were low as compared to base nickel alloy. The weld contained carbides and oxides.

Xiawei Yang, et al. [61] used ABAQUS software to study the finite element modelling of the FW (linear) of GH4169 alloy. The temperature distribution of the process was studied through the developed 2D thermo-mechanical model. The authors experimentally studied the micro, macro and axial shortening of the friction-welded joints. The friction time increased the heat conduction in the materials and the flash extruded at 1.75 sec FW time. The shear stress during the welding was major up to the welding time of 0.75 sec. Through the microstructures, the presence of the fine-grained structures was found at the flash and the weld interface zones. Yanni Wei et al. [62] utilized a continuous drive FW machine to join aluminium and copper at different welding conditions. Joint performance was studied through SEM, EDS and X-ray diffraction (XRD) techniques. There was no defect found. The temperature at the weld interface during the welding was in the range of 375-450°C. CuAl<sub>2</sub> and Cu<sub>9</sub>Al<sub>4</sub>

phases were found in the joints through EDS and XRD. This research proved the prediction of Cu-Al phases through the Gibbs free energy model.

Stinville, J.C. et al. [63] did the welding of a Ti-6Al-4V titanium alloy plate using the linear FW process and studied the fatigue behaviour of a similar joint. The report said that the crack propagation and nucleation were not found in the weld interface and the Thermomechanical Affected Zone (TMAZ), but it happened in the base metal region which was mainly by the welding conditions. According to the fatigue conditions, the fracture occurred where the accumulation of strains was higher and the maximum strain accumulation was found in the TMAZ. Daniela Ramminger Pissanti et al. [64] did the FW of S32205 stainless steel (pipe girth). They studied the microstructure and Charpy v-notch test at 0°C temperature. The results showed a modification in the microstructures which depended on the plastic deformation formed and the high temperature. There was a reduction in the impact strength of the joint due to the formation of ferrite and the changes in the austenite phase in the microstructure. The fractography study showed the cleavage fracture in the impact-tested specimen. According to Xujing Nan et al. [65], the maximum entropy production principle called MEPP can be used for the development of a 2D finite element model with the use of DEFORM software in the joining of GH4169 super alloy by continuous drive FW process. The effect of friction pressure and linear speed in the process was observed. The results showed that less frictional time was required when the linear speed was approximately 2.0 m/s and the friction pressure increased. The transition temperature was higher than the recrystallization temperature.

Yu Su et al. [66] linear-friction welded the titanium alloy (Ti-6Al-2Zr) and studied the joint performance through microstructure and mechanical properties. The results showed that the grains were refined due to the thermo-mechanical effect. There was a difference in the microstructure of the base metal and the weld zone. The strength was higher in the weld zone than that of the base metal as the breakage happened at the base metal during the tensile testing. Further, the impact energy absorption of the joint was also increased by 19% when compared to the base titanium alloy. Carlos Alexandre Pereira de Moraes et al. [67] did a comparative study of residual stress assessment between the FW (FW) and gas tungsten arc welding (GTAW). For this, the metal API 5L X65 pipe girth was welded by both gas-tungsten arc welding and FW and each of them gave distinct residual stresses. To find the residual stresses X-ray diffraction was used and a microhardness and microstructure study was done on the weld specimen. It was noted that there was no porosity in the joint prepared by FW, but some porosity was found in the joints by the GTAW. The microhardness was increased and lower residual stresses were found in the FW joint and these are vice

versa in the GTAW joint with heterogeneous microhardness.

According to Ramsey, F. Hamade et al. [68], generally, plastic pipes are being joined by the fusion process and showed the improvement in the plastic pipe joining by friction heating process with good joining quality. The author compared the advantages of FW over the butt welding fusion process in joining plastic pipes. In the case of energy consumption, rotary FW showed almost one-tenth less compared to butt welding. So, the impact of FW on the environment and from an economic point of view was understood. Ho Thi My Nu et al. [69] studied the joining of a similar Ti-6Al-4V titanium alloy, which was a high-strength alloy, through the rotary FW process. The authors indicated the significance of the rotary FW of this titanium alloy as the fusion welding yielded poor properties. They developed a thermo-mechanical model to predict the temperature gradients while welding. The strength of the friction-welded Ti-6Al-4V joint was greater compared to the base alloy. The upset can be produced in titanium welding by the higher forging pressure. This research recommended having small forging pressure during the rotary FW process.

Xiangjun Xu et al. [70] studied the feasibility of the FW process on the alloy TiAl (high Nb). The microstructure and tensile properties were evaluated. All the weld joints had a transition zone between the severely deformed zone and the parent or base metal in the range of a few microns. The joint's tensile strength was higher than that of base metal. The bi-concave lens geometry formation was identified through the microstructure. According to the fractography, the fracture took place in the base metal with a brittle fracture. The grain size increased with the increase of distance from the sever-deformed zone. Selvamani S.T. et al. [71] joined low chromium carbon AISI 52100 steel by FW and studied the corrosion behaviour. Plain carbon steel can be replaced by this kind of metal, so the frictional joining of this steel is needed in the automobile industry. An empirical relation was developed for the ease of predicting the optimized parameters. The friction pressure (FP) was more than that of forge pressure (FOP) about 0.5 MPa/sec time and these parameters produced a maximum notch tensile strength of 710 MPa. The results showed that the chuck rotational speed had much more effect on the tensile strength followed by FP and FOP. The small grains of 11 µm showed a maximum hardness of about 310 HV. Further, the electrochemical impedance showed 72% of charge transfer for the welded joints.

#### 4. FW OF DISSIMILAR METALS

One of the most notable advancements in FW research is its application to dissimilar materials. This development has opened up new possibilities for joining materials with vastly different properties,

enabling the creation of hybrid structures that optimize the strengths of each material. Researchers have made significant strides in understanding the challenges and solutions for dissimilar FW, making it an invaluable process for industries requiring such combinations. The literature stated the need for joining dissimilar metals and described the research with different material combinations like aluminium to stainless steel, carbon steel to aluminium, steel to copper alloys, aluminium to copper alloys, aluminium to magnesium, and carbon steel to stainless steel etc. [72]. The possibility of joining alumina composite with AA6061 alloy by the FW is proved through the study conducted and the study inferred that the interface was thick and had a mixture of silicon (Si), magnesium (Mg), and aluminium (Al) oxide [73]. However, the plastic deformed zone (FPDZ) zone, which is a contrast to the deformed zone (DZ), was identified in the weld interface. Wei Guo et al. [74] did a study on joining 7A04 aluminium alloy and AZ31 magnesium alloy dissimilar welding by inertia FW (IFW). The intermetallics  $Al_{12}Mg_{17}$  and  $Al_{13}Mg_2$  were identified in the weld interface and their layer thickness was decreased in micron size ( $\mu m$ ) when increasing FP. According to Andrzej Ambroziak et al. [75], in the dissimilar joining of steel with aluminium, the fragile intermetallic leads to weld degradation. Emel Taban et al. [11] confirmed the formation of Al-Fe intermetallics related to FeAl and  $Fe_2Al_5$  through their investigation of joining AA6061 alloy with AISI1018 steel. The effects of softening on AA6063 and hardening on AA5052 were identified through their research and also proved that the pressure reduction narrowed down the thickness of the softened HAZ. Maximum tensile strength of 250 MPa was achieved.

Zhida Liang et al. [76] evaluated the FW feasibility of joining pure Aluminium-1060 and AZ31B Magnesium dissimilar joints. The performance of the joints was characterized by microstructures and mechanical tests. During the experiments, forge and friction pressures were varied and 2800 rpm speed and 10 sec friction time were constant. The Al-Mg intermetallics like  $Mg_2Al_3$ ,  $Al_{12}Mg_{17}$  etc. were found at the interface region, and intermetallic phases were not benefiting to improve the properties of the joints. The increase in friction and forging pressure decreased the thickness of the intermetallic. If the thickness of the intermetallic layer was higher, then it weakened the strength of the bonding. A tensile strength of 138 MPa was obtained as a maximum with 77% joint efficiency. Meisnar M et al. [10] proved in their research that the possibility of joining dissimilar FW with no intermetallics compounds (IMC) and having the grain refinement and elongation in the vicinity of weld interface when did research on joining AA6082 and Ti-6Al-4V for aerospace applications. The study showed the possibility of residual stress in solid-state welding also. Javed Akram et al. [15] welded dissimilar metals P21 and SS304 and analysed the creep behaviour of the joints. Through their work, they implied that a

transgranular mode of fracture was observed and the damage was mainly due to the cavity growth. Muralimohan.CH et al. [77] did work to joint stainless steel and titanium with electroplated Ni interlayer through the FW process. The results showed a decrease in interlayer thickness when FT increased and the TS increased with the increase of UP. The fracture study on the tensile-tested samples showed a brittle mode.

Feng Jin et al. [52] experimented on the DDFW of SUS304 in the diameter of  $\phi 25$  mm at 80 MPa. A 2D finite element analysis (FEA) model was constructed to simulate the thermo-mechanical coupling during welding. The results show that the corona bond develops and fills out the interface, in which the temperature is rising. Alloy 42CrMo steel and Ni-based superalloy K418 were joined by inertia FW by Yuhan Ding et al. [78]. Intermetallic compounds and carbides like NbC and TiC were found at the interface with a diffusion layer. Rajesh Jesudoss Hynes and Shenbaga Velu P [79] welded alumina and steel with an aluminium interlayer and developed a numerical model to study the thermo-mechanical behaviour of the weld. Zhida Liang et al. [76] studied the continuous drive FW of AZ31B magnesium alloys to AA5A33 aluminium alloys and reported that the tensile strength was increased with the increase of friction time (5 sec) and the formed intermetallics improved the hardness of the joints. Radosław Winiczenko [12] achieved 87% joint efficiency when joining AISI1020 with A536 dissimilar alloys, in the study the author found the diffusion of carbon from iron to steel through EDS. The significance of the process is a small amount of the base metal is heated and that which is melted is thrown from the joint, therefore, the intermetallic material is kept to a very minimum. Prasanthi et al. [26] successfully welded Mild steel with a titanium rod of  $\phi 10$ mm x100mm using the FW process. Through the study, they confirmed the formation of a fine FeTi intermetallic phase at the weld interface and the hardness value of 350 VHN at the interface was obtained. Kundu.S and Chatterjee.S [80] welded titanium and SS304 alloys with 'Ni' interlayer. Through their research, it was identified that the Ni interlayer did not block the diffusion of Titanium to the stainless steel side. In their study, the strength of a weld joint would drop with an increase in joining temperature because of the formation of Fe-Ti brittle intermetallic.

A broad investigation was performed by Xinyu Wang et al. [81] on Ti-6.5Al-3.5Mo-1.5Zr-0.3Si titanium alloy joined by linear FW (LFW). The results showed that friction pressure refines the grains in the weldment efficiently and the sound LFW joint is not possible at low shear velocity, but it is possible to reduce the width of the Thermo mechanically-affected zone (TMAZ) by friction pressure, and shear velocity. Marlon A. Pinheiro and Alexandre. Q. Bracarense [17] studied the influence of the surface contact geometry (faying modifications) of joining Al.6351/1020 steel through FW and accepted that the geometry on the



contact pin would influence the mechanical properties. Alloy 42CrMo steel and Ni-based superalloy K418 were joined by inertia FW by Yuhan Ding et al. [78]. Intermetallic compounds and carbides like NbC and TiC were found at the interface with a diffusion layer. Nanotechnology research is about depositing nanolayer films on specimens to reduce defects during FW [82]. Many explorations have been tried in FW with the interlayer. When TiNi alloy is welded to stainless steel, a large amount of brittle Fe<sub>2</sub>Ti intermetallics, which is brittle, at the weld interface, would be formed [32]. Fu Li and Du Suigeng [34] studied the performance of molybdenum and die alloy dissimilar joints through a continuous drive FW process and obtained defect-free joints with good strength. The authors identified the grain refinement near the weld interface. Jeswin Alphy James and Sudhish. R [14] studied the effect of interlayers in the frictional joining of AISI304L and AISI1040 dissimilar alloys. The research concluded that the nickel interlayer increased the tensile strength with maximum burn-off length and decreased the hardness at the weld interface. The reason behind the hardness reduction was the chromium carbide precipitation by nickel.

Hazman Seli et al. [24] developed a thermo-mechanical finite element model to evaluate the friction-welded alumina/mild steel dissimilar joints. In this research, the AA6061 sheet was used as an interlayer to improve the bonding strength. Through the model, the temperature distribution was simulated and the highest deformation, strain and stress were found in the heat-affected zone of the joint. The FW can be successfully used for the joining of composite materials. Rotundo. F et al. (2013) [83] studied the dissimilar welding of aluminium matrix composite (AA2124 aluminium alloy + 25% by Vol. silicon carbide particles) and the AA2024 aluminium alloy using an FW machine. The prepared joint quality was analysed and the results showed that no blending was found between composite and aluminium alloy and the mechanical testing also proved that the frictional joining was feasible for the composite metal joining with good weld properties. Further, it was noted that the addition of silicon carbide particles in the composite restricted the plastic flow and the fracture happened near the TMAZ region of the weld joint. Peng Li et al. [84] did research to weld copper and alumina dissimilar metals with AA1100 aluminium interlayer through a continuous/direct drive FW process. The tensile strength of the joint, microstructures at the interface and fracture of joints were evaluated. The results showed that micro cracks were available in the weld zone due to the thermo-mechanical coupling and the joints with good bonding. The authors found that 12 MPa friction pressure and 12 sec friction time were the optimized parameters providing maximum strength. The pure aluminium interlayer improved the strength and bonding by

increasing the wettability during FW. The failure took place at the alumina and pure aluminium interface.

It was a tough task of welding high-density (16-17 g/cm<sup>3</sup>) tungsten heavy alloy and low-density (2.7 g/cm<sup>3</sup>) aluminium dissimilar alloys. Radoslaw Winiczenko et al. [85] frictionally welded aluminium alloy with tungsten heavy alloy and studied the micro and mechanical performance of the joints. Around 84 % of joint efficiency was achieved maximum with good bonding. Friction pressure of 40 MPa and 3.5 sec. friction time showed maximum strength. It had to be noted that the increase of friction pressure increased the tensile strength of the joint and gradually decreased after reaching the maximum level. No intermetallic was found at the weld interface except the Fe-Ni element enrichment and no diffusion of tungsten into the aluminium side was found. Tran Hung Tra and Motoki Sakaguchi [86] fabricated the friction-welded dissimilar joint of metals Inconel-718 and M247 and analysed the fatigue property of the joint. The fracture happened in the M247 base metal instead of the joint. The joint showed good strength and properties under high cycle at 700°C. Jian Luo et al. [18] joined high carbon steel (HCS) with brass metal through inertia FW. The character of the weld interface was analysed. Some weld defects like trench-shaped holes were in the joint. The holes were formed due to the insufficient frictional effect. The phases with copper (Cr) and iron (Fe) compounds were found in the weld interface. Longwei Pan et al. [23] frictionally (Rotary) joined aluminium and copper metals. The maximum strength and elongation obtained through this research were 88 MPa and 20%. As mentioned in some of the literature, the strength of the joint could be reduced due to the wide thickness of intermetallic. Fractography showed the net-like fracture at the centre of the tensile fractured samples. Most of the intermetallic formed during the FW were CuAl<sub>2</sub> and Cu<sub>9</sub>Al<sub>4</sub>. It was further mentioned in this article that the preheating temperature could decrease the strength and elongation and increase intermetallic thickness.

Peng Li et al. [87] fabricated the titanium (TC4 alloy) with 316L steel dissimilar joints through rotary FW. The structure and mechanical characterisation were done on the welded joints with and without post-heat treatment. A different interface was found i.e. the concave and convex shapes were formed at 316L and TC4 alloy sides. The results showed that the post-weld heat treatment highly increased the value of tensile up to a maximum of 419 MPa as compared to the strength of 117 MPa for the joints without heat treatment. Some of the intermetallic like Fe<sub>2</sub>Ti, AlTi<sub>3</sub>, Fe-Ti, and FeNi<sub>3</sub> were found at the weld interface and decreased the weld strength. The brittle cleavage fracture mode was observed during the fracture analysis. The post-heat treatment helped attain a homogeneous structure in the weld. Radhakrishnan. E et al. [19] studied the FW between the C44300 alloy tube and the AA7075 alloy tube plate. They studied the hardness and strength of the joint with and threading on the tube plates. The

results showed that the compressive strength was higher for the joint with thread. The rotation speed led to having better weld strength than other parameters. The sample with low speed produced maximum hardness at the weld interface. The microstructure study showed fine grain refinement and good bonding at the interface. The threaded joint had no defects. This study helped consider the effect of different friction rotational speeds on mechanical and microstructure characterisation during the FW of joining dissimilar tubes and tube plates.

Mumin Sahin [22], did research on the dissimilar joining of aluminium and copper through the FW process at 60 MPa friction pressure on 10 mm diameter rods and found that the axial shortening of the aluminium side was more than the copper side through the macro and microstructures examination; this was mainly due to the low melting point of aluminium than copper. Thus, the aluminium metal expelled more flash. The elongated grain near the weld interface of the aluminium side was also found. The brittle intermetallic  $Fe_3Al$  was further found in the aluminium zone. It further showed the mixed layer of fracture with brittleness on the aluminium side during the tensile testing. Maximum tensile strength of 140 MPa was obtained through this research. Pandiarajan.S et al. [88] welded the metals SA213 (tube) and SA387 (tube plate) by friction welded process as per the L9 orthogonal array and found that the welded joints had no defects. Microstructure and mechanical properties were studied. The authors experimented with two modes; one was with holes and another one was without holes on the circumference of the tubes. The results showed that the projection of the tube during the welding was the most influencing factor and identified the fine grains near the weld interface. The joint without holes on the circumference showed higher hardness and strength compared to that of joints with holes. Rajesh Jesudoss Hynes and Shenbaga Velu. P [89] welded the titanium Ti/6Al/4V alloy with AA6061 aluminium alloy by rotary FW and studied the effect of the speed of weld specimen rotation. The results found an increase in the friction heat at the centre of the joint while the rotational speed increased. The equiaxed grain structure was formed in the joint. Phases like TiAl and  $Ti_3Al$  were found at the interface. It was stated that a speed of 100 rpm was needed to attain improved strength and impact toughness.

Efe Isik and Cicek Ozes [90] successfully welded (rotary friction) the hot-forged steel tube yoke with cold-drawn steel tube (thin-walled) available in automobiles. This is considered a dissimilar frictional joining from an application point of view as both components are different and as per the manufactured method of steel. A maximum of 553 HV was achieved along the weld joint and the fatigue life of the joint was estimated at 220 cycles at a 72 MPa shear stress. The least strength was less than the base alloy of about 13%. The heat-affected zone length of the tube yoke side was less than the tube side (2 mm). Kimura. M. et

al. [30] studied the frictional joining effect on the tensile strength of the friction-welded joint of nickel-based super-alloy and heat-resistant steel. The results showed that there was no crack in the joint and the effect of welding parameters on the dissimilar joint. The phenomenon of the joining process was identical for both friction pressures 30 MPa and 90 MPa. When the forge pressure was equal to the friction pressure in the process, it did not show 100% joint efficiency during the welding, but 100% joint efficiency was achieved for 3 sec. friction time with 360 MPa forge pressure. It was identified that the nature of the weld region whether softened or hardened depends on the friction time.

From an application point of view, FW is more helpful. Yoshihiko Hangai et al. [91] fabricated AA1050 aluminium tubes filled with Al-Si-Cu alloy foam by the FW process. During the welding process, no deformation was found on the metal. The holding time and the holding temperature of the foaming process influenced the sound tube fabrication. The suggested holding time and temperature were about 510 sec. and 675°C. Senthil Kumaran.S et al. [92] predicted the tensile value of friction-welded dissimilar joints made of SA387 tube plate and SA213 tube. This research confirmed the possibility of welding tube plates with a tube in a fast and easy manner without defects. The input parameters considered for the joining were a projection of the tube, rotational speed, and depth of cut, and the strength was the output parameter. From the results obtained, it was informed that the grain refinement in the weld zone improved the tensile strength of the joint with a maximum of 839 MPa. The genetic algorithm was used for the prediction and the deviation between the obtained value and the experimental value were minimal. Yingping Ji et al. (2016) [93] welded the dissimilar titanium alloys Ti-6Al-4V Ti-5Al-4Mo-4Cr-2Sn-2Zr through FW (linear) and studied their microstructure and mechanical properties of the joints. Microstructures showed that the larger grain refinement and the smaller grains were found in the weld zones than in the thermo-mechanically affected zone. The strength of the joint was higher than the base alloy. The failure happened at approximately a 1.20 mm distance from the weld joint line. The fracture study showed a mixed pattern of trans. and intergranular fracture in the weld joint. The impact toughness was recorded as a minimum for the weld joint having the mixture fracture than the base weld metal having transgranular fracture mode.

Stefano Rossi et al. [94] studied the corrosion-fatigue behaviour of the friction-welded dissimilar joints made of ASTM A105-AISI304 alloys. This study acts as a tutorial for developing an effective set-up for the corrosion-fatigue behaviour study. The results showed the effect of cathodic protection on fatigue behaviour improvement. The failure analysis stated that the failure happened in the plastic zone of the weld interface itself instead of at the parent metal. Packiaraj Rajendran et al. [95] studied the tensile,



hardness and axial shortening of the friction-welded dissimilar joints of low-carbon steel and tool steel. The study informed that the maximum strength obtained was 341 MPa which was higher than the base metals. The microhardness was increasing on the tool steel side 2 mm distance away from the weld joint. Brittle intermetallic formed reducing the hardness and the strength and the fracture also showed the brittle mode. Rajesh Jesudoss Hyne. N et al. [96] proposed a numerical simulation in the FW process to study the joining phenomenon of ceramics with pure metals or alloys. This simulation was mainly to analyse (finite element) the thermal behaviour of the joints based on the heat generated during the process. It was suggested that the aluminium metal sheets could be applied to improve the wettability nature of the FW and the analysis was done at different interlayer thicknesses. The results showed that the increase in thickness reduced the heat-affected zone of the joint and increased the strength with maximum efficiency.

## 5. FW OF ALUMINIUM AND STAINLESS STEEL

Aluminium is a non-ferrous metal; stainless steel mainly consists of Nickel, Chromium; lastly, iron is burse ferrous metal. It is difficult to weld both dissimilar metals by traditional welding techniques due to their different chemical metal compositions. The research was done on the weld feasibility test and showed that it is possible to weld aluminium with stainless steel using rotary friction welding (RFW) with no scar, no defects and a narrow heat-affected zone. As aluminium is a soft material, there is the penetration of stainless steel (hard metal) into the soft metal.

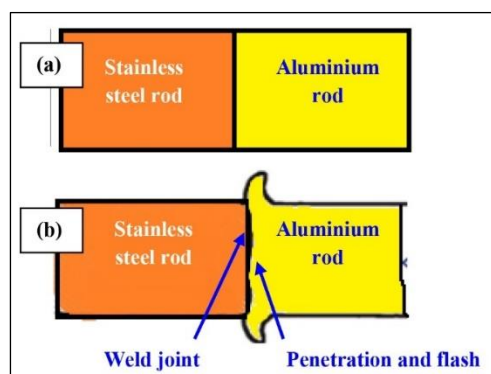


**Fig. 3.** Overlap penetration of AISI304L into AA6063 soft alloy during dissimilar RFW joint: a) before penetration with frictional force; b) penetration due to frictional effect [9]

In figure 3 (a, b), it is shown that the penetration that usually happens during the FW of aluminium with stainless steel and with excess metal as a flash comes out. Yong Liu et al. [97] did research on aluminium/stainless steel dissimilar metals with IFW

and found that an intermetallic compound layer (IMC) was developed at the joining interface of the weld, and a thicker IMC layer was observed while increasing rotational speed. Kimura et al. [2] joined aluminium 6063 and stainless steel 304 dissimilar alloys through the FW process and achieved 100% efficiency with good joints. Honggang Dong et al., [5] studied the linear growth of the  $Fe_4Al_{13}$  phase in the joining of 5052 aluminium alloy and 304-stainless steel by rotary FW with post-weld heat treatment.

The intermetallic compound formations can be reduced with the application of interlayers. When Nickel (Ni) interlayer is used it changes the microstructure at the weld interface area and improves the joint strength. Many trials ended up improving the dissimilar weld strength like welding with a compatible interlayer [7], [98] introduced in between both the metals during DDFW, which, in turn, is called three-element FW. Kannan P et al. [99] studied the effect of silver interlayer in the joining of AA6061 metal matrix composite with AISI304 by FW. Through the research, the authors reported that the Ag interlayer decreases the particle fracture and frictional coefficient.



**Fig. 4.** AISI304L/AA6063 dissimilar RFW joint: a) before machining; b) after machining [9]

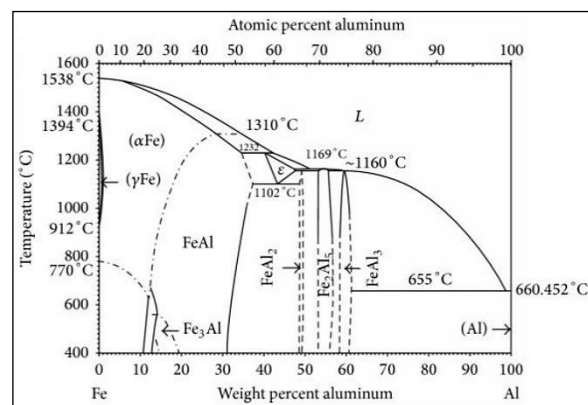


**Fig. 5.** Aluminium-iron binary diagram [100], [101]

Kumar. R and Balasubramanian. M [31] stated that the copper interlayer also can impart excellent bonding during FW and it prevents the martensitic stages in HAZ which is narrow. Figure 4 shows the dissimilar joint of AA6063 (non-ferrous aluminium) and AISI304L (ferrous austenitic stainless steel) alloys. The welding specimens of dia.  $\phi 12$  mm were 100 mm in length each and finally, the dissimilar

weldment (after RFW) had a length of 175 mm. Around 24 mm was noted as material loss/axial shortening. Figure 5 shows the Fe-Al binary phase diagram [100, 101] that is having intermetallic. According to Xiaolin Li et al. [102], at Al-rich in the phase diagram, the complex intermetallic compounds available are FeAl, Fe<sub>5</sub>Al<sub>8</sub>, FeAl<sub>2</sub>, Fe<sub>2</sub>Al<sub>5</sub>, and Fe<sub>4</sub>Al<sub>13</sub>.

Mantra Prasad Satpathy et al. [103] did a study on joining Aluminium 3003 alloy and AISI304 steel alloy sheets using a copper interlayer employing a solid-state welding process. The results showed that superior plastic deformation and microhardness are higher in the parent metal than in the weld zone. The interfacial failure occurred in the weld interface, which failure was dependent on friction time.

Suresh D. Meshram et al. [7] joined AA6061 and AISI4340 by the FW with a silver (Ag) interlayer and proved that Ag replaced Fe<sub>2</sub>Al<sub>5</sub> intermetallic and magnesium content in the aluminium side thus reducing the width of the intermetallic layer and increasing tensile strength. The introduction of the nickel interlayer improves the mechanical property by replacing the Fe<sub>2</sub>Ti phase [32]. Kimura M et al. [28] worked on the joining of aluminium (pure) to SS304 steel and evaluated the tensile strength and the bend ductility of the joint. Through that study, it is observed that the maximum joint efficiency was obtained at about 80% as 100% could not be possible due to the decrease in tensile strength of pure aluminium. The weld interface temperature reached a maximum with an increase in friction time. The maximum temperature on the weld interface was about 300°C at 2 sec. friction time during FW. The main intermetallic developed when joining aluminium (Al) and stainless steel (SS) dissimilar metals are FeAl (Fe rich), FeAl<sub>2</sub>, Fe<sub>3</sub>Al, FeAl<sub>16</sub>, Fe<sub>2</sub>Al<sub>5</sub> (Al. rich), Fe<sub>2</sub>Al<sub>3</sub>, and FeAl<sub>3</sub>. These intermetallic may weaken the weld strength, thus it is necessary to choose the welding technique which is suitable for improving the weld quality by reducing the intermetallic formation and narrowing the HAZ.

Hardik Vyas et al. [104] joined aluminium 6063 and stainless steel 304L dissimilar pipes through a continuous drive FW process. They found that there was no crack or defects in the welded joints. The enormous aluminium flash was developed by the large deformation due to the frictional force. The method yielded 60% joint efficiency and 15% elongation at 350 rpm.

Karthik. G. M. et al. [105] introduced a new buttering method in their research of joining austenitic stainless steel and Al-Cu-Mg alloy. It was reported that the buttering method showed its effect on the performance of the joint and it eased the joining of metals.

Madhusudhan G. Reddy et al. [6] studied the influence of Cu, Ni and Ag interlayers formed by the electroplating process in the joining of aluminium 6061 with stainless steel (SS) 304 by direct drive FW process. The authors mentioned that the combination of aluminium and stainless steel is widely used in

spacecraft and cryogenic applications and welding of both metals was not possible by fusion welding. The results showed that the Ag interlayer produced a strong and ductile joint compared to others. The reason was Ni and Cu interlayer formed the NiAl<sub>3</sub> and CuAl<sub>2</sub> brittle intermetallic at the weld interface and the Ag stopped the development of Fe<sub>2</sub>Al<sub>5</sub> intermetallic in the AA6061/SS304 dissimilar joint.

Frictional force in the form of stirring may be used in the preparation of dissimilar lap joints. Raju Prasad Mahto et al. [106] studied the effect of friction stir-lap welding in joining AA6061 and AISI304 alloys. The results showed that the quasi-cleavage fracture was found at the low joining speed, but the ductile fracture mode was shown through SEM images when the speed was at maximum. The micron-level intermetallic like Al-Fe and Al<sub>5</sub>Fe were confirmed by point energy dispersive spectroscopy (EDS). The main benefit of this friction stir-lap welding was the generation of low heat near the weld region which in turn reduced the intermetallic thickness. The fractures happened outside the weld interface.

According to Reddy Prasad K and Sridhar V.G [107], FW is advisable in the welding of dissimilar alloy combinations like aluminium and steel. The heating profile on the aluminium side is huge in the joining of aluminium alloy with stainless steel; this is because of the high thermal conductivity of aluminium. The heat generation is involving directly the quality of the weld prepared, and it is the combination of friction pressure, rotational speed and FW time. Shubhvardhan R.N and Surendran.S [108] joined aluminium 6082 with AISI304 metals through the FW process at the parameters 80 MPa friction pressure, 5 sec. friction time, 1500 rpm rotational speed, upset time (5 to 8 sec.) and upset pressure (150 to 300 MPa). The tensile and impact energy observations were studied in addition to the microstructural analysis. The tensile strength obtained was the maximum of 192 MPa. The results showed the initial increase in joint strength while increasing upset time and upset pressure gradually decreased. A maximum of 12 J was achieved at the 180 MPa upset pressure. It was also mentioned that the upset times tried in this study could not generate the required heat for the joining at the upsetting phase. The accumulation of FeAl intermetallic at the joint interface had reduced the strength.

Eder Paduan Alves et al. [109] studied the temperature gradients during the FW of AA1050 and AISI304L alloy using a thermocouple data logger at low pressures of about 2.1 MPa and 52 sec. AA1050 is pure aluminium and commercially available with a soft nature. Through this research, they found that the maximum temperature at the weld interface was about 375°C and further announced that the heating rate reached the maximum in the first 10 seconds of the welding process.

Honggang Dong et al. [110] studied the rotary FW of AA5052 alloy and AISI304 alloy. The

microstructure and mechanical characterizations were studied. The formations of phases  $\text{Fe}_4\text{Al}_{13}$ , and  $\text{Fe}_2\text{Al}_5$  were found. The centre and edge locations of the weld joints were analysed. The brittle intermetallic was not developed in the centre of the joint, but the phases with more thickness were identified towards the edges near the weld flash from the centre, 99.5% of joint efficiency was obtained. The heat-affected zone was thinner on the AISI304 side rather than the side of the AA5052 alloy. The fracture study stated that the failure was there in the R/4 location from the centre with a brittle fracture.

## 6. INFLUENCE OF FW PARAMETERS

Friction and upset pressures, and friction time, upset time and the rotating speed, burn-off length are the FW parameters that dominate the microstructural and mechanical properties of the welded joints [111] and they are varied for optimizing the welding process to get a strong joint [112]. According to Peng Li et al. [113], initially, the required process parameters have to be selected by the try-and-error method in the rotary FW process and the authors developed a model and the mathematical expressions for estimating the heat generation at the weld interface during the rotary FW process. When operating with high friction pressure, the quantity of the released heat, as well as extruded metal heat, is also increasing [114]. Serdar Mercan et al. [115] evaluated the influence of FW parameters when joining AISI2205 alloy with AISI1020 alloy. According to them, if the welding parameters are selected correctly considering the materials to be welded and the geometrical dimension of the weld specimen, then they would improve the performance of the weld joint. However, during the FW of aluminium and steel, there is some possibility of forming a thin layer of brittle intermetallic compounds [116]. Friction time, upset time, burn-off length and speed are the parameters controlling the FW efficiency [8]. For instance, the creation of  $\text{FeAl}_3$  brittle IMC may be controlled by increasing the speed [29, 117].

Kimura M et al. [2] studied the importance of friction time (FT) in joining AA6063 with SS304 at friction pressure 30 MPa and concluded that when friction time increases the weld interface temperature also increases, which in turn softens the weld interface. Peak temperature and cooling rate play a vital role since they influence the residual stress in the welded joint. Some trial was also tried by Ajith P.M et al. [118] to weld S32205 duplex stainless steel and the study said that the percentage contribution of input parameters, for instance, upset pressure (47%) and friction pressure (27%) were dominating majorly. Rupinder Singh et al. [119] have done work on joining dissimilar polymer materials with FW. The maximum values were obtained at 1200 rpm and for 4 sec time. Paventhan R et al. [120] welded AA6082 alloy and AISI 304 dissimilar joints with FW and found through response surface methodology (RSM) that friction

pressure had a greater influence on the tensile strength of joints followed by friction time. Bennett C [121] researched inertia FW on CrMoV alloy and concluded that when high pressure was used for the welding, the HAZ width was reduced. Changbao Song et al. [122] analysed atomic diffusion behaviour, plastic deformation, and temperature change while welding between titanium (Ti) based alloys with linear FW. Their investigation revealed that the deformed area of the welded zone was increased with the increase of friction time and also Ti showed higher diffusion ability than that of Aluminium. Friction time substantially affects the quality of the weld.

Adrian Lis et al. [123] did work on linear FW with 250 Hz oscillation frequency for joining AA5052 and AA6063 and found that the sound joint was achieved at 30 MPa friction pressure and discussed the importance of frictional time. The effects of softening on AA6063 and hardening on AA5052 were identified through their research and also proved that the pressure reduction narrowed down the thickness of the softened HAZ. Kimura M et al. [2] identified that if the heating time increases then the weld interface becomes thicker. Interface temperature increases with FT while joining by FW, it was noted that the heating time increases the flash of the joint. In the joining of A6063/304SS materials, the efficiency of friction welded joints increased with the increase of FT, but the efficiency and the bending ductility can be improved by the UP. The friction pressure (FP) shows a direct effect on the tensile strength (TS) of the AISI 1020-ASTM A536 joint but upset force decreases the TS. When FP increased, the value of TS also increased. There is a possibility to increase TS by increasing friction time (FT) [12]. During the joining of pure Al. and pure Fe with DDFW, there was a formation of a discontinuous layer in the interface and the TS increased with the increase of pressure.

An extensive investigation was performed by Xinyu Wang et al. [81] on Ti-6.5Al-3.5Mo-1.5Zr-0.3Si titanium alloy joined by linear FW (LFW). The results showed that friction pressure refines the grains in the weldment efficiently and the sound LFW joint is not possible at low shear velocity. It is possible to reduce the width of the Thermomechanical Affected Zone (TMAZ) by friction pressure, and shear velocity.

Gawhar and Sherko [3] joined 316L steel to 1045 steel and the fracture took place near the thermo-mechanically affected zone (TMAZ), but the author discussed that the forge pressure increases the hardness. Palanivel. R et al. [124] investigated the effect of welding parameters on the tensile strength of friction-welded titanium tubes. From their research, it was known that the rotational speed influences the weld flash and the weld zone geometry. The size and the ring shape of the flash were increased with the increase in speed. The amount of deformed metal was increased due to the increase in rotational speed, which in turn plasticized the material and increased the material ejection. The higher speed reduced the grain

size and improved the hardness. The friction time increased the size of the weld zone. In this titanium frictional joining, the grain size was further reduced and tensile strength increased when the friction time increased.

Peng Li et al. [84] stated in their research that when the friction pressure and friction time increased the tensile strength of the dissimilar joint (copper-pure aluminium-alumina) and the optimized welding parameters were obtained.

Raji Reddy et al. [125] strongly mentioned that FW process parameters must influence the weld quality. The authors did a study on the influence of FW parameters on the impact toughness while joining preheated 15CDV6 alloy. The maximum toughness value was achieved as 53 Joule and the preheating process also helped improve the toughness value. The parameters upset force and the burn-off length showed more effect on the joint toughness.

Romero, J et al. [126] studied the effect of forging pressure in the joining of titanium alloy (Ti.6AL.4V) through the linear FW process and found the relationship between forging pressure and the residual stress developed during welding. Forging pressure showed its effect in the generation of weld alpha-titanium element texture along the weld line. If the forge pressure is low the texture is strong. Weld zone width and the development of residual stress were decreased with the increase of forging pressure. The research also confirmed the decrease in weld temperature when the pressure increased.

Marjan Safarzadeh et al. [16] studied the effect of friction rotational speed on the properties of composite (Alumina+ Mullite) and aluminium 6061 alloy dissimilar joints. It was noted that the fracture propagates along the cleavage planes at low frictional speed whereas the dimple structure was formed at high speed and the higher rotational speed improved the bending property and the hardness of the friction welded joints.

Uday. M. B et al. [73] tried to join 25%, and 50% alumina ( $Al_2O_3$  ceramic) reinforced yttria-stabilized zirconia with aluminium 6061 alloys using an FW machine. For joining, rotational speed was maintained from 900 to 1800 rpm, friction pressure was constant at 7 MPa, and the friction time was 30 sec. The microstructure and mechanical properties were evaluated. The results showed that the strength of the joint was good at the low rotational speed. The rate of deformation was high on the Al.6061 side. The rotational speed during FW increased the frictional heat between the weld surfaces and showed changes in the interface thickness. Further, the speed increased grain refinement. The bending strength could be increased at a low speed and the joint specimen of a low percentage of alumina showed the maximum bending strength. The effect of the rotational speed was thoroughly understood through the performance of the joint. As per the research done by Zhou, Y et al. [127] using FW, the welding parameters were influencing the

mechanical properties of the various similar and dissimilar joints like AA6061-AA6061 alloy, Al.6061-matrix composite (AMC)-AA6061 combination, AMC-AMC. Notch tensile strength and fatigue strength of the joints were evaluated. The friction pressure showed its effect on the tensile property of all the joints, but upset pressure showed its effect only on the notch tensile strength of the joint with the AA6061-AA6061 alloy combination. The variation in friction time did not affect the notch tensile strength values of any joint. The dissimilar combination had lower-notch tensile strength compared to others. The fatigue strength of frictionally welded joints was low as compared to the base metals.

Chennakesava R. Alavala [4] studied the influence of parameters in the frictional joining of AA2024 alloy with SS304. The ANSYS analysis software was used in this research to the weldability through the finite element method. The parameters considered were friction pressure, friction time, forging pressure and rotational speed. Here, the ratio of forging pressure ( $P_{fo}$ ) and the friction pressure ( $P_f$ ) was above the one of 1.25, 1.5, and 1.7. The bulk deformation decreased when the forge pressure increased and the rotational speed increased. The research further stated the importance of the  $P_{fo}/P_f$  ratio and its influence on the property of the joint and the friction time and rotational speed were also influencing the process.

Deepak Mani and Ananthapadmanaban.D [128] studied the mechanism of FW between aluminium and stainless steel and mentioned that friction pressure was more important in improving tensile strength. The thickness and type of the intermetallic phases formed during the welding at the weld interface can also influence the strength of the joints and it was reported that  $Fe_2Al_5$  was the common phase during the welding between aluminium alloy with 304 austenitic stainless steel.

Palanivel. R et al. [129] studied the mechanical and microstructure properties of friction-welded titanium tubes. Through this research, it was confirmed the significance of FW in joining thin tubes. It was stated that the speed of the weld specimen in the chuck showed its effect on the weld bonding and the microstructure. While the chuck rotation increased, the frictional torque production decreased and this phenomenon thus increased the welding time. It was informed that the higher rotational speed improved the fine grain refinement in the centre of the weld joint rather than the coarse grain in the outer region of the joint near the flash. The grain sizes of 2.5  $\mu m$  and 1.2  $\mu m$  were obtained for the speeds of 1600 rpm and 2800 rpm, respectively. An increase in speed decreased grain size. Similarly, maximum microhardness was achieved at the speed of 2800 rpm. There was no change in the formation of the grains between the heat-affected zone and the parent zone in the weld joint. A maximum of 98% weld efficiency was obtained for the maximum rotational speed. From the research, it could be understood that the rotational speed parameter was one

of the important parameters that affected the weld properties.

Normally, optimization is common among FW. Sreenivasan. K.S et al. [130] used the genetic algorithm (GA) technique to optimize the FW parameters in joining aluminium matrix composite (AA7075 + 10% SiC particles). They studied the effect of process parameters on the hardness and the tensile strength of the joint. The optimized parameters were equal to 1490 rpm, upset and friction pressure 209 MPa and 98 MPa respectively. The maximum strength reached a value of 244 MPa. The GA optimization was confirmed by the experimental results. The mixed mode of ductile and brittle fracture was observed in the tensile-tested samples.

Mariane Chludzinski et al. [131] produced higher outer diametric API 5L X46 pipe girth joints through the FW within less time. There were no defects found. The mechanical properties were decreased at the centre. The results showed the possibility of hydrogen cracking and brittle fracture with the MnS phase.

Deep Barua et al. [132] proposed the joining of a circular bar or tube with a metal plate or sheet metal through the FW process. The work has to be appreciated from an application point of view. In this work, the effectiveness of process parameters like feed rate, rotational speed, frictional torque and the depth of penetration on the property of the joint has been discussed. According to the results, the frictional torque played a major role in the development of the required heat for the joining. An increase in the rotational speed of the spindle reduced the torque developed and the axial thrust. When feed increased, the torque was also increased.

Wei Liu et al. [133] studied the upset prediction on the friction-welded joints using a neural network. It is an appreciated method and it can be applied to both rotary and linear FW processes. The predicted values were compared to the finite element method simulation results. It was proved that the heat source depended on the rotation speed and the axial frictional pressure

usually affects the accumulation of the heat at the weld joint. The error was calculated as less than 8%. While considering the coefficients of correlations for rotary and linear FW processes were 0.998 and 0.963 respectively.

Guilong Wang et al. [134] studied the effect of energy on the mechanical properties of the 304 stainless steel rotary friction-welded joint. The welding time was varied in the range of 4 to 20 sec at the pressure range of 25 to 200 MPa. The forging pressure was maintained above the friction pressure during the rotary FW of AISI 304 alloy. It was observed that the increase in the energy input increased the tensile strength of the joint at the constant forging pressure (170 MPa). An empirical model was created to optimize the parameters and compared with the experimental values and the accuracy of the model was confirmed by checking of tensile strength coefficient which was in the range of 90- 96%.

Fuqiang Lai et al. [135] studied the effect of inertia FW process parameters for the 42Cr9Si2 engine valve. It was confirmed that the excellent weld joint fabrication relied on the selection of optimized weld parameters and their values. The recommended upset pressure and friction weld pressure were the maxima of 10.3 MPa and 10.0 MPa. After the durability test, the crack was not identified in the friction welded part.

Table 2 discusses the tensile strength, peak load by the weld joint and the axial shortening during the friction welding process which was done at different welding parameter combinations. When the friction pressure increases, it is to be noted the increase in strength and peak load. It was noted that when the FP increases then the joint efficiency also increases.

Figure 6 shows the formation of excess metal as weld flash and the dissimilar joining during the RFW. It was observed that if the heating pressure increases then the joint changes according to the input of forces due to that heating pressure and then the quantum of weld flash also increases, as shown in the figures.

**Table 2.** Influence of FW parameter on mechanical properties and metal loss [136]

Experimental parameters in RFW			Results obtained					
FP (Bar)	UP (Bar)	FT (sec)	Tensile (MPa)	Joint efficiency (%)	Axial shortening (mm)	Vickers hardness at the weld zone (Hv0.3)		Toughness (J)
						SS304L	Al.6063	
12	18	3	154	71.6	13.7	286	52	32
12	21	5	159	73.9	19.1	285	50	34
12	24	7	156	72.5	19.5	278	45	34
15	18	5	167	77.6	21.8	289	47	36
15	21	7	165	76.7	23.6	276	48	38
15	24	3	163	75.8	18.1	308	45	36
18	18	7	186	86.5	26.9	282	47	36
18	21	3	178	82.7	20.5	314	47	32
18	24	5	189	87.9	25.0	288	48	36

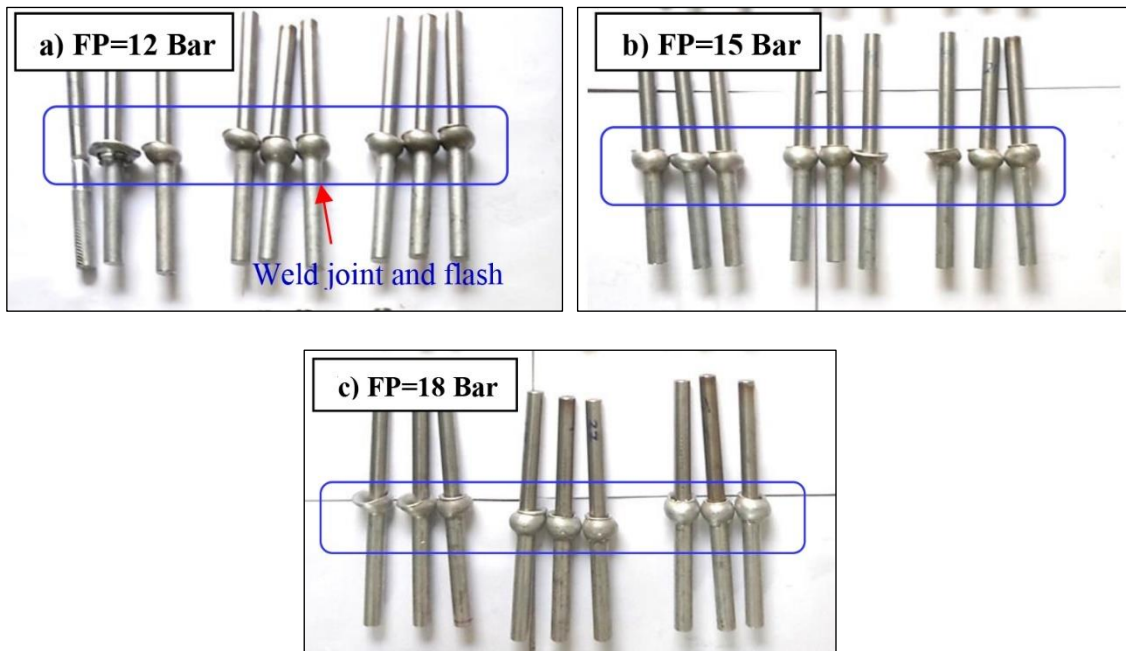


Fig. 6. Weld flash variation according to friction pressure (FP) [136]

## 7. INFLUENCE OF FP AND FAYING SURFACE MODIFICATIONS IN FW

The influence of friction pressure and faying surface modifications in rotary friction welding is a critical aspect of the welding process. FW has proven to be a highly effective and versatile welding process with a wide range of applications across industries such as aerospace, automotive, and energy. Its unique ability to create strong, reliable joints while minimizing heat-affected zones and distortion makes it an attractive choice for many engineering applications. It is necessary to have an improvement in the properties of the welded joints fabricated by rotary friction welding. The welding parameters and the faying surface modifications dominate the properties of the prepared joints as they influence the joints' performance. For research, the weld joints were prepared by Senthil et al. [9, 138, 139] between aluminium and stainless steel at different welding conditions and faying surface modifications on the weld specimens. It was found through the characterization techniques that the properties were not uniform for all the joints and the properties were varied based on the friction welding parameters and the faying surface modifications. The parameters like friction pressure, friction time, axial feed rate, and upset pressure were important. When the friction pressure increased it increased the tensile strength and in turn improved the joint efficiency of the welding trials. It was found that the higher friction pressure caused the higher axial shortening. Similarly, the higher friction time sometimes damages the joint and reduces the properties by softening the region near the weld interface of the soft material AA6063 side. A higher feed rate of the stationary part onto the rotary part during friction welding improves the tensile

strength and increases the axial shortening. By controlling the FP and feed rate, the axial shortening can be controlled to stop material loss. The level of FP applied affects the amount of heat generated at the faying surfaces. Higher pressure can lead to increased heat generation, which, if not controlled properly, could potentially lead to material overheating or excessive flash formation. The upset time and upset pressure were responsible for the fineness of the grains near the weld joints.

The tapered faying surfaces on the AISI304L specimen improved the bonding between the weld specimens and the tensile strength of the dissimilar joint, but it also increased the axial shortening of the joining trial. The surface modifications on the AISI304L specimen improved the strength of the AA6063 specimen. The coating on the weld specimen by dipping process needed much more friction time for the bonding to take place with high friction pressure. Similarly, the deep recess method also needed more friction time to have good bonding. The tapering on both the weld materials stimulated the attachment between the materials during friction welding. The geometrically shaped faying surface modifications could be able to improve the microhardness property nearby the weld interface since these modifications hardened the weld region by pushing the huge force created by the frictional effect through the friction welding process; however, it slightly reduced the impact strength of the joints. The modifications with the interlayers through the electroplating process on the AISI304L specimen improved the strain hardening behaviour and the hardness of the joint, but the axial hardening and elongation of the joint were low (except 'Cr' interlayer) [137].



The threaded faying surfaces improved the microhardness near the weld interface. It also improved the joint efficiency; anyhow, no further improvement was identified in elongation and impact strength. The joining methods with hemispherical faying surfaces were far better in improving the properties of the weld joints especially strength, strain hardening & hardness etc. There was a difference in the properties of the joints prepared by the methods having the surface modifications on the AISI304L specimen only and the methods having the surface modifications on both AA6063 and AISI304L specimens. Table 3 shows the various geometrically modified faying surfaces used for FW research in dissimilar joining. The joint efficiency or joint quality factor was calculated by the ratio of the strength of the joint to the strength of the soft base metal. Here, the soft base metal is AA6063, and its TS value is considered 215 MPa which is used for the joining efficiency calculated. The joint was done with 18 bar friction pressure and 24 bar upset pressure with 5 sec. friction time. From the results, the authors mentioned that by changing the

faying surfaces, the strength and properties can be increased. The joint efficiency of geometrically modified experiments was compared with the experiment without modification (flat faying surfaces) as shown in the table. The axial shortenings observed during the welding process of the joints with different faying surfaces (A to H) are given in Figure 7.

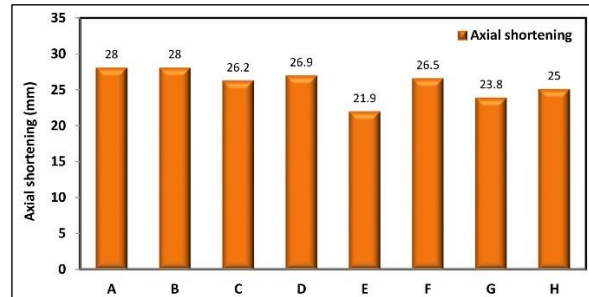
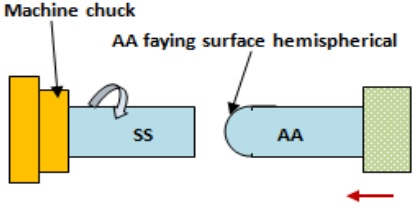
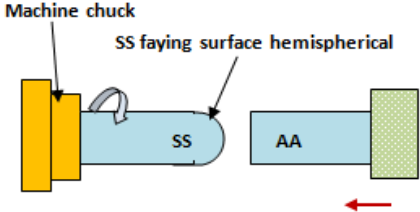
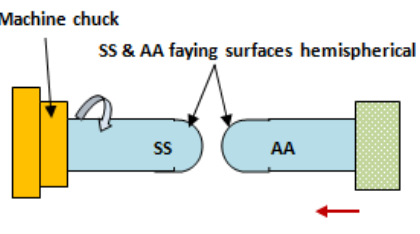
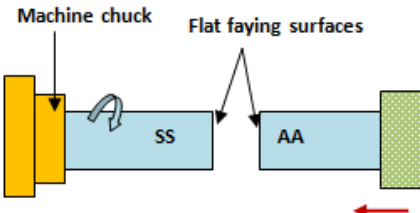


Fig. 7. Axial shortening of joints with various faying surfaces joints

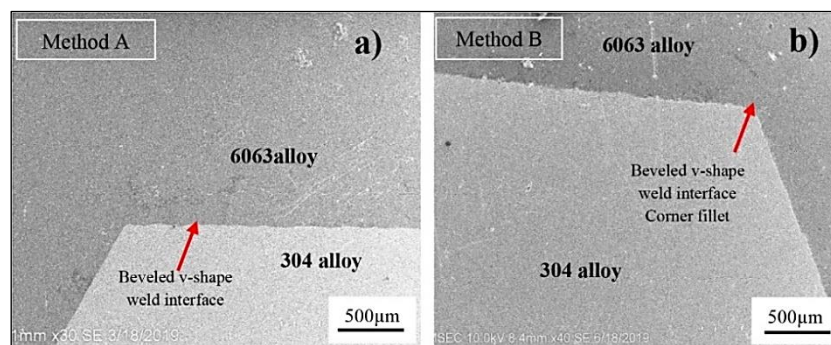
Table 3. Some of the geometrically modified faying surfaces for dissimilar FW [9, 138, 139]

Faying surface-modified RFW B/W AA6063 and SS304 alloys (Methods)	Description	Joining efficiency (%) achieved
<p><b>A</b></p>	FW of AA6063 (AA) specimen with faying-surface tapered AISI304L (SS) specimen. d1=12 mm, d2= 6 mm.	94.7
<p><b>B</b></p>	FW of AA6063 (AA) specimen with faying-surface tapered AISI304L (SS) specimen. d1=12 mm, d3= 9 mm.	101.0
<p><b>C</b></p>	FW of faying-surface recessed AA6063 (AA) specimen with faying-surface tapered AISI304L (SS) specimen. d1=12 mm, d2= 6 mm.	94.5
<p><b>D</b></p>	FW of both faying-surfaces tapered (1:1/2 ratio of dia.) AA6063 (AA) & AISI304L (SS) specimen. Where, d1=12 mm, d2= 6 mm.	102

Faying surface-modified RFW B/W AA6063 and SS304 alloys (Methods)	Description	Joining efficiency (%) achieved
 <p><b>E</b></p>	<p>RFW of flat AISI304L (SS) specimen with hemispherical (half portion spherical) faying-surfaced AA6063 (AA) specimen. Dia. of rod= 12 mm.</p>	<p>97</p>
 <p><b>F</b></p>	<p>RFW of flat AA6063 (AA) specimen with hemispherical faying-surfaced AISI304L (SS) specimen. Dia. of rod = 12 mm.</p>	<p>109.7</p>
 <p><b>G</b></p>	<p>RFW of hemispherical faying-surfaced both AISI304L (SS) &amp; AA6063 (AA) specimens. Dia. of rod = 12 mm.</p>	<p>110.6</p>
 <p><b>H</b></p>	<p>FW of AA6063 (AA) specimen with AISI304L (SS) specimen without any modification.</p>	<p>87.89</p>

Surface modifications that improve adhesion and wettability between materials can lead to a more uniform and desirable microstructure at the interface. This can result in better joint performance and mechanical properties. Figure 8 (a to h) confirms the weld interface developed between the alloys 6063 and 304 by the methods A to H respectively. The weld interface has no defects and it changed according to the faying surfaces selected. The 'V' and 'C' curved WI can be seen, which provides a large weld interface

contact area between the dissimilar alloys. It is proved that the faying surface modifications increase the contact area and the strength by developing plastic deformation. Higher FP tends to lead to greater plastic deformation at the faying surfaces. This increased deformation can result in grain refinement within the microstructure. Excessive FP can generate more heat at the faying surfaces, potentially causing a wider heat-affected zone (HAZ) in the base materials.



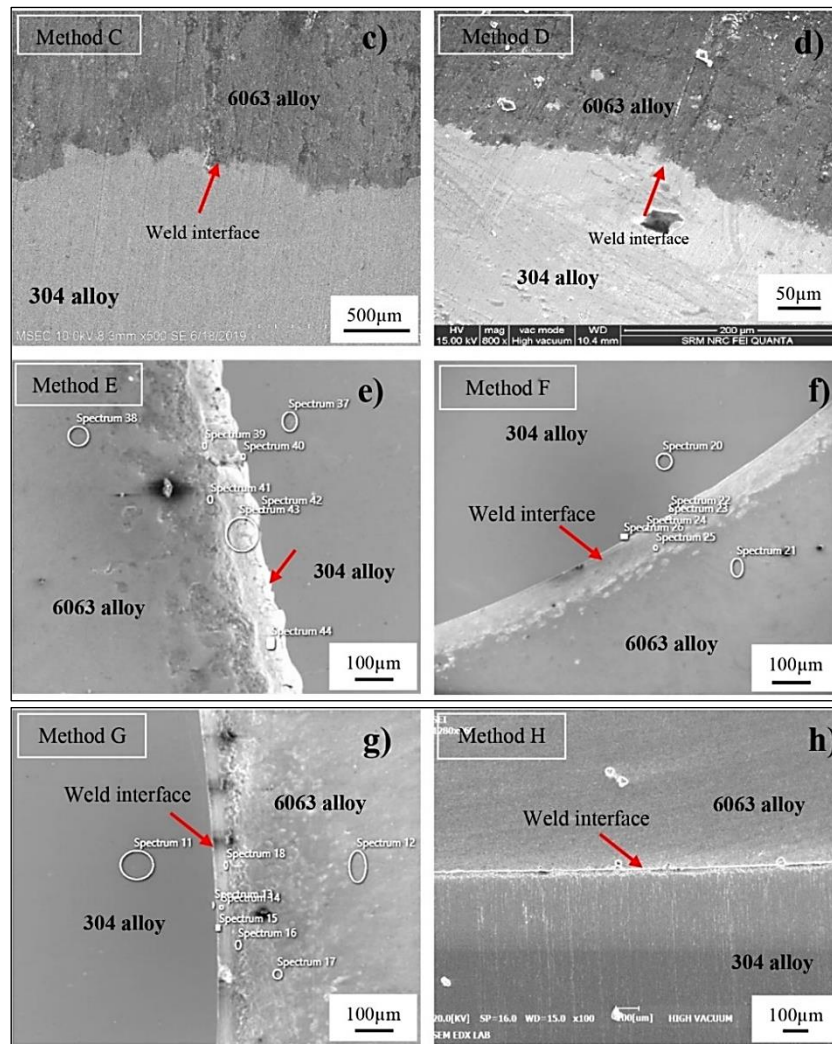
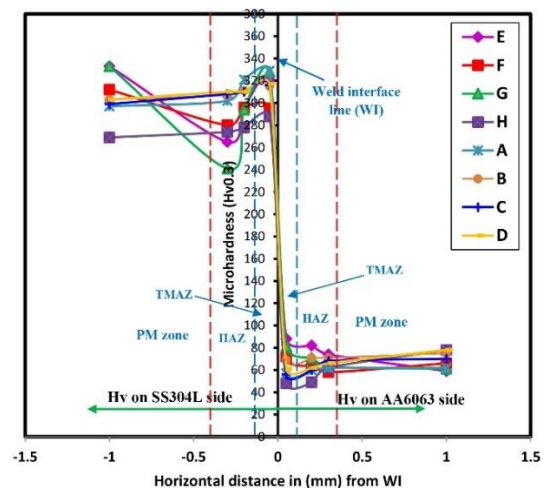


**Fig. 8.** Microstructures of the AA6063-SS304 alloy weld joint with different faying surfaces [9, 139]

The results of microhardness on both sides of the AA6063-SS304L alloy friction weld joint [138, 139], which were fabricated with different faying surface modifications (Methods A-H, Table 3) were analysed and are shown in figure 9.

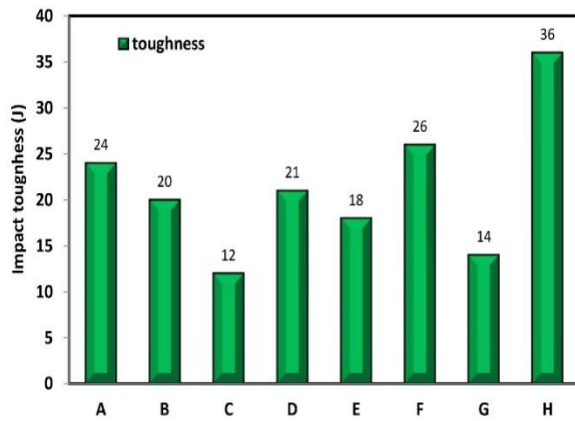
The graph shows the hardness values on both sides (soft and hard metals) of the joints in HV 0.3 with 10 sec. dwell time. The values were measured from the zones of the hardness specimens like the weld zone that consists of weld interface (WI), thermo-mechanically affected zone (TMAZ) ( $\leq \pm 0.1\text{mm}$  in figure 9), heat affected zone (HAZ) ( $\leq \pm 0.25\text{mm}$  in figure 9) and parent metal (PM). The measurement was taken from WI (centre axis in figure 9) towards PM ( $\geq \pm 0.5\text{mm}$ , figure 9) on both sides separately.

From the results, it was observed that the microhardness was higher near WI on the 304 side and it was higher near PM on the 6063 sides as the metal near the WI on AA6063 was affected by FP and led to softening during the FW.



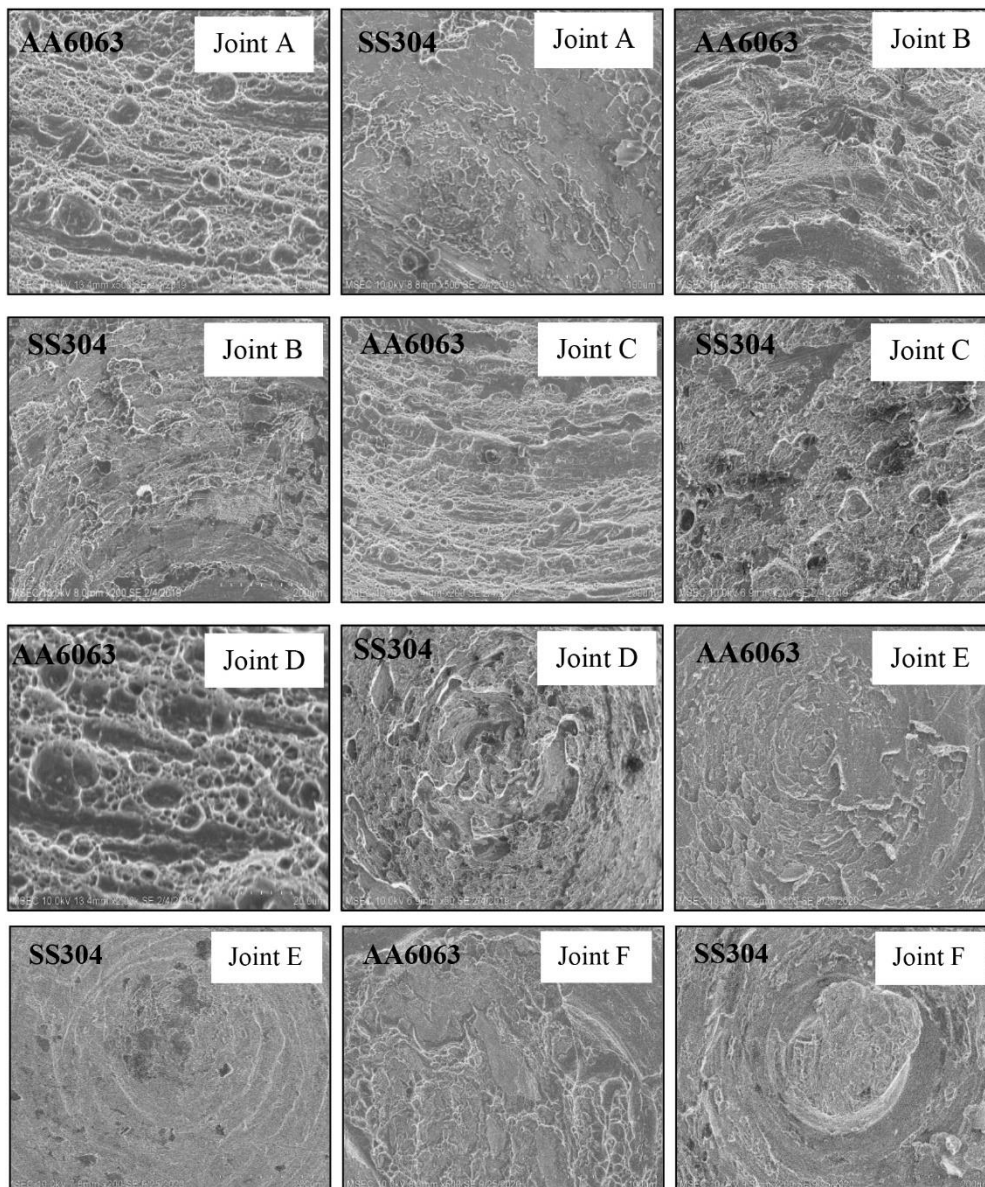
**Fig. 9.** Vickers' hardness measurement on both sides of the AA6063/SS304L FW joint prepared by different joining methods (A-H) from the weld interface (WI) line.





**Fig. 10.** Impact toughness for the welded joints through joining methods A-H

The values were the maximum of 340 HV and 80 HV on 304 and 6063 sides respectively. Methods B, C and D were good hardness. Method A has the highest hardness value near the WI of the SS304L side. The toughness values of 6063/304L dissimilar joints are given in Figure 10. The values are in the range of 12J to 36J depending on the faying modifications. It is confirmed that the faying surface design can change the impact strength of the joint. The joint without weld surface modifications showed better impact toughness than the joint with weld surface modifications because the softness developed in specimen H during the impact test led to more impact ductility. It is necessary to analyse the fracture of the impact-tested specimens which are shown in figure 11 for both AA6063 and SS304 sides. Figure 12 is the specimen after the impact test.



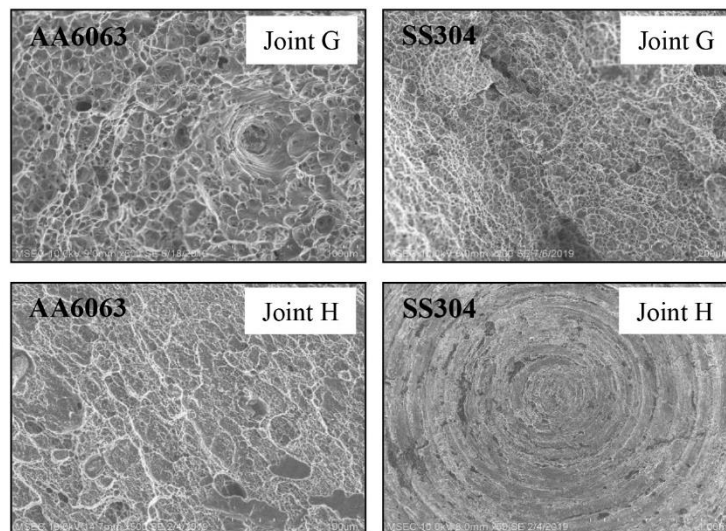


**Fig. 11.** Impact fracture images of both sides of all joints A to H [9, 138, 139]

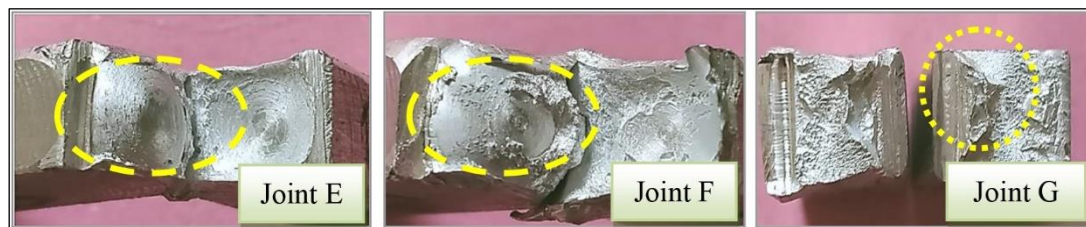


**Fig. 12.** Impact fractured specimen with semi-spheroid faying surfaces [139]

The influence of FP and faying surface modifications in rotary friction welding is crucial for achieving high-quality welds. Balancing the pressure to optimize both weld strength and energy efficiency is essential. Additionally, proper surface preparation and, when necessary, surface modifications can enhance the weldability of materials and ensure the integrity of the joint. This knowledge is vital for engineers and technicians involved in rotary friction welding processes, as it allows them to tailor the parameters to specific applications and materials, resulting in strong, reliable, and efficient welds. Faying surface modifications are particularly important in dissimilar material welding. Surface treatments or coatings can help bridge the gap in material properties and improve the bond between dissimilar materials.

## 8. CONCLUSIONS

This review of FW research has shed light on the significant influence of this innovative joining technique in various industries and its continuous development to address both similar and dissimilar welding scenarios.

From the survey, it is agreed that FW is quite good for joining aluminium alloys with other metal combinations (ferrous/ nonferrous/ceramic). As the demand for joining low carbon content ferrous alloy with heat treatable non-ferrous alloy of small diameter

rods in industries increases and no literature addressed the direct-drive FW with small diameter rods with low FP, constant welding research is still needed.

Further, some work reported that the frictional joining could be done with minimum axial shortening, minimum energy utilization, and safety precautions for the welding operators by handling low welding pressure conditions and without damaging the weld specimen during the FW. To our knowledge, no such solid-state welding (by continuous drive FW) method was tried before for joining steel AISI304L and aluminium AA6063-T6 rods having small diameters for the dissimilar joining at low FP and UP with different faying surfaces and the research is still limited.

It is further noted that if the axial penetration rate and upset time rise, the strength of the welded joint might increase. The faying surface modifications can influence the mechanical properties of the weld similar/dissimilar joints, WI and alter the microstructures.

A research work exhibited that some of the faying surfaces reduced the FT during FW. The joining methods with hemispherical bowl faying modifications showed better tensile properties with more than 100% joining efficiency with these parameters selected. Though such new faying surface designs improve tensile strength, an improvement in other mechanical properties cannot be said without proper research.

The application of modelling, numerical and computational analysis like structural and thermal distribution analysis on the welded joint interface during the friction welding process is still lacking.

**Conflict of Interest:** The authors declare that no conflict of interest.

**Funding Agencies:** No funding was provided for this study.

## REFERENCES

- [1] **Manideep D., Balachandar K.,** *Welding Parameters-Metallurgical Properties Correlation of Friction Welding of Austenitic Stainless Steel and Ferritic Stainless Steel*, Journal of Applied Sciences, Vol. 12, pp. 1013-1019, 2012, 10.3923/jas.2012.1013.1019.
- [2] **Wang G. L., Li J. L., Wang W. L. et al.,** *Rotary friction welding on dissimilar metals of aluminum and brass by using pre-heating method*, International Journal of Advanced Manufacturing Technology, Vol. 99, pp. 1293 - 1300, 2018, <https://doi.org/10.1007/s00170-018-2572-y>.
- [3] **Gawhar I. K., Baban S. A.,** *Efficiency of Dissimilar Friction Welded 1045Medium Carbon Steel and 316L Austenitic Stainless Steel Joints*, Journal of Materials Research and Technology, Vol. 8(2), pp. 1926-1932, 2019, <https://doi.org/10.1016/j.jmrt.2019.01.010>.
- [4] **Chennakesava R. Alavala,** *Weldability of Friction Welding Process for AA2024 Alloy and SS304 Stainless Steel using Finite Element Analysis*, International Journal of Engineering Research and Application, Vol. 6 (3), pp. 53-57, 2016.
- [5] **Dong H., Yang J., Li Y., Xia Y., Hao X., Li P., Sun D., Hu J., Zhou W., Lei M.,** *Evolution of interface and tensile properties in 5052 aluminium alloy/304 stainless steel rotary friction welded joint after post-weld heat treatment*, Journal of Manufacturing Processes, Vol. 51, pp. 142-150, 2020, <https://doi.org/10.1016/j.jmapro.2020.01.038>
- [6] **Madhusudhan G. Reddy, Sambasiva A. Rao, Mohandas.T.,** *Role of Electroplated Interlayer in Continuous Drive Friction Welding of AA6061 to AISI 304 Dissimilar Metals*, Science and Technology of Welding and Joining, Vol. 13. iss.7, pp. 619-628, 2008, <https://doi.org/10.1179/174329308X319217>.
- [7] **Meshram S. D., Madhusudhan Reddy G.,** *Friction Welding of AA6061 To AISI 4340 Using Silver Interlayer*, Defence Technology, Vol. 11, pp. 292-298, 2015, <https://doi.org/10.1016/j.dt.2015.05.007>.
- [8] **Kannan P., Balamurugan K., Thirunavukkarasu K.,** *Influence of Silver Interlayer in Dissimilar 6061-T6 Aluminum MMC and SS304L Stainless Steel Friction Welds*, The International Journal of Advanced Manufacturing Technology, Vol. 81, 2015, pp. 1743-1756, 10.1007/s00170-015-7288-7.
- [9] **Senthil Murugan S., Noorul Haq A., Sathya P.,** *Effect of welding parameters on the microstructure and mechanical properties of the friction-welded dissimilar joints of AA6063 alloy and faying surface-tapered AISI304L alloy*, Welding in the World, Vol. 64, pp. 483-499, 2020, <https://doi.org/10.1007/s40194-020-00846-x>
- [10] **Meisnar M., Baker S., Bennett J. M., Bernad A., Mostafa A., Resch S., Fernandes N., Norman A.,** *Microstructural Characterisation of Rotary Friction Welded AA6082 and Ti-6Al-4V Dissimilar Joints*, Materials and Design, Vol. 132, 2017, pp. 188-197, <http://dx.doi.org/10.1016/j.matdes.2017.07.004>.
- [11] **Taban E., Gould J. E., Lippold J. C.,** *Dissimilar Friction Welding of 6061-T6 Aluminium and AISI 1018 Steel: Properties and Microstructural Characterisation*, Materials and Design, Vol. 31, 2010, pp. 2305-2311. <https://doi.org/10.1016/j.matdes.2009.12.010>.
- [12] **Winiczenko R.,** *Effect of Friction Welding Parameters on the Tensile Strength and Microstructural Properties of Dissimilar AISI 1020-ASTM A536 Joints*, The International Journal of Advanced Manufacturing Technology, Vol. 84, 2016, pp. 941-955, 10.1007/s00170-015-7751-5.
- [13] **Kimura M., Choji M., Kusaka M., Seo K., Fuji A.,** *Effect of friction welding conditions on mechanical properties of A5052 aluminium alloy friction welded joint*, Science and Technology of Welding and Joining, Vol. 11(2), 2006, pp. 209-215, 10.1179/174329306X89242.
- [14] **James J. A., Sudhish R.,** *Study on Effect of Interlayer in Friction Welding for Dissimilar Steels: AISI304L and AISI1040*, Procedia Technology, Vol. 25, 2016, pp. 1191-1198, <https://doi.org/10.1016/j.protcy.2016.08.238>.
- [15] **Akram J., Kalvala P. R., Misra M., Creep I. C.,** *Behaviour of Dissimilar Metal Joints Between P91 and SS 304*, Materials Science and Engineering A, Vol. 688, 2017, pp. 396-406. <http://dx.doi.org/10.1016/j.msea.2017.02.026>.
- [16] **Safarzadeh M., Mohd Nor A. F., Basher U. M.,** *Effect of Friction Speed on the Properties of Friction Welded Alumina-Mullite Composite to 6061 Aluminium Alloy*, Journal of the Australian Ceramic Society, Vol. 52(2), 2016, pp. 134-142. [www.austceram.com/ACS-journal](http://www.austceram.com/ACS-journal).
- [17] **Pinheiro M. A., Bracarense A. Q.,** *Influence of Initial Contact Geometry on Mechanical Properties in Friction Welding of Dissimilar Materials Aluminum 6351 T6 and SAE 1020 Steel*, Advances in Materials Science and Engineering, 1759484, 2019, <https://doi.org/10.1155/2019/1759484>.
- [18] **Jian Luo, Junfeng Xiang, Dejia Liu, Fei Li, Kelian Xue,** *Radial Friction Welding Interface between Brass and High Carbon Steel*, Journal of Materials Processing Technology, Vol. 212, 2012, pp. 385-392, 10.1016/j.jmatprotec.2011.10.001.
- [19] **Radhakrishnan E., Kumaraswamidhas L. A., Palanikumar K., Muruganandam D.,** *Strength and Hardness Studies of C44300 Tube to AA7075-T651 Tube Plate Threaded and Unthreaded Dissimilar Joints Fabricated by Friction Welding Process*, Journal of Materials Research and Technology, Vol. 8(4), 2019, pp. 3424-3433, <https://doi.org/10.1016/j.jmrt.2019.06.008>.
- [20] **Hong Ma, Guoliang Qin, Peihao Geng, Fei Li Banglong Fu, Xiangmeng Meng,** *Microstructure Characterisation and Properties of Carbon Steel to Stainless Dissimilar Metal Joint Made by Friction Welding*, Materials and Design, Vol. 86, 2015, pp. 587-597, <https://doi.org/10.1016/j.matdes.2015.07.068>.
- [21] **Sahin M.,** *Joining of Stainless-Steel and Aluminium Materials by Friction Welding*, The International Journal of Advanced Manufacturing Technology, Vol. 41, 2009, pp. 487-497, <https://doi.org/10.1007/s00170-008-1492-7>.
- [22] **Sahin M.,** *Joining of Aluminium and Copper Materials with Friction Welding*, The International Journal of Advanced Manufacturing Technology, Vol. 49, 2010, pp. 527-534, <http://dx.doi.org/10.1007/s00170-009-2443-7>.
- [23] **Longwei Pan, Peng Li, Xiaohu Hao, Jun Zhou, Honggang Dong,** *Inhomogeneity of Microstructure and Mechanical Properties in Radial Direction of Aluminum/Copper Friction Welded Joints*, Journal of Materials Processing Technology, Vol. 255, 2018, pp. 308-318. <https://doi.org/10.1016/j.jmatprotec.2017.12.027>
- [24] **Hazman Seli, Mokhtar Awang, Ahmad Izani Md. Ismail, Endri Rachman, and Zainal Arifin Ahmad,** *Evaluation of Properties and Fem Model of the Friction Welded Mild Steel-Al6061-Alumina*, Materials Research, Vol. 16(2), 2013, pp. 453-467, 10.1590/S1516-14392012005000178.
- [25] **Seli H., Ismail A. I. Md., Ranchman E., Ahmad Z. A.,** *Mechanical Evaluation and Thermal Modelling of Friction Welding of Mild Steel and Aluminium*, Journal of Materials Processing Technology, Vol. 210, 2010, pp. 1209-1216, <https://doi.org/10.1016/j.jmatprotec.2010.03.007>.
- [26] **Prasanthi T. N., Sudha C., Ravikiran S., Naveen Kumar N., Janaki Ram G. D.,** *Friction Welding of Mild Steel and Titanium: Optimization of Process Parameters and Evolution of Interface Microstructure*, Materials and Design, Vol. 88, 2015, pp. 58-68, <http://dx.doi.org/10.1016/j.matdes.2015.08.141>.
- [27] **Akram J., Kalvala P. R., Chalavadi P., Mishra M.,** *Dissimilar Metal Weld Joints of P91/Ni Alloy: Microstructural Characterization of HAZ of P91 and Stress Analysis at the Weld Interfaces*, Journal of Materials Engineering and Performance, Vol. 27, 2018, pp. 4115-4128, <https://doi.org/10.1007/s11665-018-3502-8>.
- [28] **Kimura M., Suzuki K., Kusaka M., Kaizu K.,** *Effect of friction welding condition on joining phenomena, tensile strength, and bend ductility of friction welded joint between pure aluminium and AISI 304 stainless steel*, Journal of Manufacturing Processes,



- Vol. 25, 2017, pp. 116-125, <https://doi.org/10.1016/j.jmapro.2016.12.001>.
- [29] **Kimura M., Fuji A., Shibata S.**, *Joint Properties of Friction Welded Joint Between Pure Magnesium and Pure Aluminium with Post-Weld Heat Treatment*, *Materials and Design*, Vol. 85, 2015, pp. 169-179. <http://dx.doi.org/10.1016/j.matdes.2015.06.175>.
- [30] **Kimura M., Nakashima K., Kusaka M., Kaizu K., Nakatani Y., Takahashi M.**, *Joining Phenomena and Tensile Strength of Joint Between Ni-Based Super-Alloy and Heat-Resistant Steel by Friction Welding*, *The International Journal of Advanced Manufacturing Technology*, Vol. 103, 2019, pp. 1297-1308, <https://doi.org/10.1007/s00170-019-03611-7>
- [31] **Kumar R., Balasubramanian M.**, *Application of Response Surface Methodology to Optimize Process Parameters in Friction Welding of Ti-6Al-4V and SS304L rods*, *Transactions of Nonferrous Metals Society of China*, Vol. 25, 2015, pp. 3625-3633, [https://doi.org/10.1016/S1003-6326\(15\)63959-0](https://doi.org/10.1016/S1003-6326(15)63959-0).
- [32] **Fukumoto S., Inoue T., Mizuno S., Okita K., Tomita T., Yamamoto A.**, *Friction Welding of TiNi Alloy to Stainless Steel Using Ni Interlayer*, *Science and Technology of Welding and Joining*, Vol. 15(2), 2010, pp. 124-130, <https://doi.org/10.1179/136217109X12577814486692>.
- [33] **Muralimohan C., Ashfaq M., Ashiri R., Muthupandi V., Sivaprasad K.**, *Analysis and Characterization of the Role of Ni Interlayer in the Friction Welding of Titanium and 304 Austenitic Stainless Steel*, *Metallurgical and Materials Transactions A*, Vol. 47, 2016, pp. 347-359, <https://doi.org/10.1007/s11661-015-3210-z>.
- [34] **Fu L., Du S.**, *On Exploring Better Friction Welding Joint of T2M Mo-Base Powder Alloy and H11 Mold Steel*, *Journal of Northwestern Polytechnical University*, Vol. 19, 2001, pp. 557-561.
- [35] **Lesniewski J., Ambroziak A.**, *Modelling the Friction Welding Of Titanium and Tungsten Pseudoalloy*, *Archives of Civil and Mechanical Engineering*, Vol. 15, 2015, pp. 142-150. <http://dx.doi.org/10.1016/j.acme.2014.06.008>.
- [36] **Donati L., Troiani E., Proli P., Tomesani L.**, *FEM Analysis and Experimental Validation of Friction Welding Process of 6xxx Alloys for the Prediction of Welding Quality*, *Materials Today: Proceedings*, Vol. 2, 2015, pp. 5045-5054, <https://doi.org/10.1016/j.matpr.2015.10.095>.
- [37] **Stütz M., Buzolin R., Pixner F., Poletti C., Enzinger N.**, *Microstructure Development of Molybdenum During Direct Drive Friction Welding*, *Materials Characterization*, Vol. 151, 2019, pp. 506-518, <https://doi.org/10.1016/j.matchar.2019.03.024>.
- [38] **Ahmed G. M. S., Algahtani A., Mahmoud E. R. I., Badruddin I. A.**, *Experimental Evaluation of Interfacial Surface Cracks in Friction Welded Dissimilar Metals through Image Segmentation Technique (IST)*, *Materials*, 2460, Vol. 11, 2018, doi:10.3390/ma11122460.
- [39] **Wei Y., Sun F.**, *Microstructures and Mechanical Properties of Al/Fe and Cu/Fe Joints by Continuous Drive Friction Welding*, *Advances in Materials Science and Engineering*, 2809356 Vol. 2018, <https://doi.org/10.1155/2018/2809356>.
- [40] **Zhu Q., Xie M., Shang X., An G., Sun J., Wang N., Xi S., Bu C., Zhang J.**, *Research Status and Progress of Welding Techniques for Molybdenum and Molybdenum Alloys*, *Metals*, 10(2), 279, 2020, <https://doi.org/10.3390/met10020279>.
- [41] **Chen X., Singh A., Kononov S., Hirsch J. R., Wang K.**, *Corrosion of Materials after Advanced Surface Processing, Joining, and Welding*, *International Journal of Corrosion*, Vol. 2018, 3569282, <https://doi.org/10.1155/2018/3569282>.
- [42] **Soares De Alcantara D., Balestrassi P. P., Freitas Gomes J. H., Carvalho Castro C. A.**, *Vibrations in CDFW*, *Entropy*, Vol. 22, 704, 2020, <https://doi.org/10.3390/e22060704>.
- [43] **Zou W., Schomburg W. K.**, *PVDF Sensor Foils Employed to Measure Shear Stress and Temperature of Friction Welding*, *Sensors*, vol. 20, 4565, 2020, <https://doi.org/10.3390/s20164565>.
- [44] **Besler F. A., Schindele P., Grant R. J., Stegmüller M. J.R.**, *Friction Crush Welding of Aluminium, Copper, and Steel Sheet Metals with Flanged Edges*, *Journal of Materials Processing Technology*, Vol. 234, 2016, pp. 72-83, <https://doi.org/10.1016/j.jmatprotec.2016.03.012>
- [45] **Faes K.**, *FRIEX: New friction welding method for automatic welding of pipelines*, *Belgian Welding Institute npo*, <https://bil-ibs.be/en/project/friex-new-friction-welding-method-automatic-welding-pipelines>.
- [46] **Aoki K., Koezawa T.**, *Characteristics of Friction Welding within a Short Time for Aluminium Alloy Deformed by ECAE Process*, *Procedia Engineering*, Vol. 207, 2017, pp. 597-602. <https://doi.org/10.1016/j.proeng.2017.10.1027>.
- [47] **Iracheta O., Bennett C. J., Sun W.**, *A Sensitivity Study of Parameters Affecting Residual Stress Predictions in Finite Element Modelling of the Inertia Friction Welding Process*, *International Journal of Solids and Structure*, Vol. 71, 2015, pp. 180-193. <http://dx.doi.org/10.1016/j.ijsolstr.2015.06.018>.
- [48] **Buffa G., Cammalleri M., Campanella D., Fratini L.**, *Shear Coefficient Determination in Linear Friction Welding of Aluminium Alloys*, *Materials and Design*, Vol. 82, 2015, pp. 238-246, <http://dx.doi.org/10.1016/j.matdes.2015.05.070>.
- [49] **Nandy S., Ray K. K., Das D.**, *Process Model to Predict Yield Strength of AA6063 Alloy*, *Materials Science and Engineering: A*, Vol. 644, pp. 413-424, <http://doi.org/10.1016/j.msea.2015.07.070>.
- [50] **Buffa G., Campanella D., Pellegrino S., Fratini L.**, *Weld Quality Prediction in Linear Friction Welding of AA6082-T6 through an Integrated Numerical Tool*, *Journal of Materials Processing Technology*, Vol. 231, 2016, pp. 389-396, <http://dx.doi.org/10.1016/j.jmatprotec.2016.01.012>
- [51] Prashanth K G, Damodaram R, Scudino S, Wang Z, Prasad Rao K, and Eckert J (2014) *Friction Welding of Al-12Si Parts Produced by Selective Laser Melting*, *Materials and Design*, Vol. 57, 632-637 <https://doi.org/10.1016/j.matdes.2014.01.026>.
- [52] **Jin F., Li J. L., Du Y., Nan X., Shi J., Xiong J.**, *Numerical Simulation Based upon Friction Coefficient Model on Thermo-Mechanical Coupling in Direct Drive Friction Welding Corresponding with Corona-Bond Evolution*, *Journal of Manufacturing Processes*, Vol. 45, 2019, pp. 595-602. <https://doi.org/10.1016/j.jmapro.2019.08.001>.
- [53] **Li P., Sun H., Wang S., Hao X., Dong H.**, *Rotary Friction Welding of AlCoCrFeNi<sub>2.1</sub> Eutectic High Entropy Alloy*, *Journal of Alloys and Compounds*, Vol. 814, 152322, 2020, <https://doi.org/10.1016/j.jallcom.2019.152322>
- [54] **Asif M., Shrikrishna K. A., Sathiya P., Goel S.**, *The Impact of Heat Input on the Strength, Toughness, Microhardness, Microstructure and Corrosion Aspects of Friction Welded Duplex Stainless Steel Joints*, *Journal of Manufacturing Process*, Vol. 18, 2015, pp. 92-106. <http://dx.doi.org/10.1016/j.jmapro.2015.01.004>.
- [55] **Sahin M., Akata H. E., Ozel K.**, *An Experimental Study on Joining of Severe Plastic Deformed Aluminium Materials with Friction Welding Method*, *Materials and Design*, Vol. 29 (1), 2006, pp. 265-274. <https://doi.org/10.1016/j.matdes.2006.11.004>.
- [56] **Raab U., Levin S., Wagner L., Heinze C.**, *Orbital Friction Welding as an Alternative Process for Blisk Manufacturing*, *Journal of Materials Processing Technology*, Vol. 215, 2015, pp. 189-192, <https://doi.org/10.1016/j.jmatprotec.2014.06.019>.
- [57] **Winiczenko R., Kaczorowski M.**, *Friction Welding of Ductile Cast Iron Using Interlayers*, *Materials and Design*, Vol. 34, 2012, pp. 444-451, <https://doi.org/10.1016/j.matdes.2011.08.038>.
- [58] **Sahin M.**, *Characterization of Properties in Plastically Deformed Austenitic Stainless Steels Joined by Friction Welding*, *Materials and Design*, Vol. 30, 2009, pp. 135-144, <https://doi.org/10.1016/j.matdes.2008.04.033>.
- [59] **Ma T. J., Chen X., Li W. Y., Yand X. W., Zhang Y., Yang S. Q.**, *Microstructure and Mechanical Property of Linear Friction Welded Nickel-Based Superalloy Joint*, *Materials and Design*, Vol. 89, 2015, pp. 85-93, <http://dx.doi.org/10.1016/j.matdes.2015.09.143>.
- [60] **Ma T., Yan M., Yang X., Li W., Chao Y. J.**, *Microstructure Evolution in a Single Crystal Nickel-Based Superalloy Joint by Linear Friction Welding*, *Material and Design*, Vol. 85, 2015, pp. 613-617, <http://dx.doi.org/10.1016/j.matdes.2015.07.046>.
- [61] **Yang X., Li W., Li J., Xiao B., Ma T., Juang Z., Cuo J.**, *Finite Element Modeling of the Linear Friction Welding of GH4169 Superalloy*, *Materials and Design*, Vol. 87, 2015, pp. 215-230, <http://dx.doi.org/10.1016/j.matdes.2015.08.036>.
- [62] **Wei Y., Li J., Xiong J., Zhang F.**, *Investigation of Interdiffusion and Intermetallic Compounds in Al-Cu Joint Produced by Continuous Drive Friction Welding*, *Engineering Science and Technology International Journal*, Vol. 19, 2016, pp. 90-95. <http://dx.doi.org/10.1016/j.jestech.2015.05.009>.
- [63] **Stinville J. C., Bridier F., Ponsen D., Wanjara P., Bocher P.**, *High and Low Cycle Fatigue Behaviour of Linear Friction Welded Ti-6Al-4V*, *International Journal of Fatigue*, Vol. 70, 2015, pp. 248-288, <http://dx.doi.org/10.1016/j.ijfatigue.2014.10.002>.

- [64] **Ramminger Pissanti D., Scheid A., Kanan L. F., Dalpiaz G Fortis Kwietniewski C. E., Pipeline Girth Friction Welding of the UNS S32205 Duplex Stainless Steel.** Materials and Design, Vol. 162, 2019, pp. 198-209, <https://doi.org/10.1016/j.matdes.2018.11.046>.
- [65] **Nan X., Xiong J., Jin F., Li X., Liao Z., Zhang F., Li J., Modeling of Rotary Friction Welding Process Based on Maximum Entropy Production Principle.** Journal of Manufacturing Processes, Vol. 37, 2019, pp. 21-27, <https://doi.org/10.1016/j.jmapro.2018.11.016>
- [66] **Su Y., Li W., Wang X., Ma T., Yang X., Vairis A., On Microstructure and Property Differences in a Linear Friction Welded Near-Alpha Titanium Alloy Joint,** Journal of Manufacturing Processes, Vol. 36, 2018, pp. 255-263, <https://doi.org/10.1016/j.jmapro.2018.10.017>
- [67] **Pereira de Moraes C. A., Chludzinski M., Menezes Nunesa R., Vieira Braga Lemos G., Reguly A., Residual Stress Evaluation in API 5L X65 Girth Welded Pipes Joined by Friction Welding and Gas Tungsten Arc Welding,** Journal of Materials Research and Technology, Vol. 8(1), 2019, pp. 988-995, <https://doi.org/10.1016/j.jmrt.2018.07.009>.
- [68] **Hamade R. F., Andari T. R., Ammouri A. H., Jawahir I. S., Rotary Friction Welding Versus Fusion Butt Welding of Plastic Pipes-Feasibility and Energy Perspective,** Procedia Manufacturing, Vol. 33, 2019, pp. 693-700, <https://doi.org/10.1016/j.promfg.2019.04.087>.
- [69] **Nu H. T. M., Le T. T., Minh L. P., Loc N. H., A Study on Rotary Friction Welding of Titanium Alloy (Ti6Al4V),** Advances in Materials Science and Engineering, Vol. 2019, 4728213, <https://doi.org/10.1155/2019/4728213>.
- [70] **Xu X., Lin J., Guo J., Liang Y., Friction Weldability of a High Nb Containing TiAl Alloy,** Materials, Vol. 12, 3556, 2019, <https://doi.org/10.3390/ma12213556>.
- [71] **Selvarmani S. T., Vigneshwar M., Palanikumar K., Jayaperumal D., The Corrosion Behavior of Fully Deformed Zone of Friction Welded Low Chromium Plain Carbon Steel Joints in Optimized Condition,** Journal of the Brazilian Society of Mechanical Sciences and Engineering, Vol. 40, 246, 2018, <https://doi.org/10.1007/s40430-018-1129-1>.
- [72] **Ma H., Qin G., Geng P., Li F., Meng X., Fu B., Effect of post-weld heat treatment on friction welded joint of carbon steel to stainless steel,** Journal of Materials Processing Technology, Vol. 227, 2016, pp. 24-33, <https://doi.org/10.1016/j.jmatprotec.2015.08.004>
- [73] **Uday M. B., Ahmad Fauzi M. N., Zubailawati H., Ismail A. B., Evaluation of Interfacial Bonding in Dissimilar Materials of YSZ-Alumina Composites to 6061 Aluminium Alloy using Friction Welding,** Materials Science and Engineering A, Vol. 528, 2011, pp. 1348-1359. <https://doi.org/10.1016/j.msea.2010.10.060>.
- [74] **Guo W., You G., Yan G., Zhang X., Microstructure and Mechanical Properties of Dissimilar Inertia Friction Welding of 7A04 Aluminium Alloy to AZ31 Magnesium Alloy,** Journal of Alloys and Compounds, Vol. 695, 2017, pp. 3267-3277. <https://doi.org/10.1016/j.jallcom.2016.11.218>.
- [75] **Ambroziak A., Korzeniowski M., Kustron P., Winnicki M., Sokolowski P., Harapińska E., Friction Welding of Aluminium and Aluminium Alloys with Steel,** Advances in Materials Science and Engineering, Vol. 2014, pp. 1-15, <https://doi.org/10.1155/2014/981653>.
- [76] **Liang Z., Qin G., Geng P., Yang F., Meng X., Continuous Drive Friction Welding of 5A33 Al Alloy to AZ31B Mg Alloy,** Journal of Manufacturing Processes, Vol. 25, 2017, pp. 153-162, <http://dx.doi.org/10.1016/j.jmapro.2016.11.004>
- [77] **Muralimohan C. H., Muthupandi V., Sivaprasad K., Properties of Friction Welding Titanium-Stainless Steel Joints with a Nickel Interlayer.** Procedia Material Science, Vol. 5, 2014, pp. 1120-1129, <https://doi.org/10.1016/j.mspro.2014.07.406>.
- [78] **Ding Y., You G., Wen H., Li P., Tig X., Zhou Y., Microstructure and Mechanical Properties of Inertia Friction Welded Joints Between Alloy Steel 42CrMo and Cast Ni-Based Superalloy K418,** Journal of Alloys and Compounds, Vol. 803, 2019, pp. 176-184, <https://doi.org/10.1016/j.jallcom.2019.06.136>.
- [79] **Hynes R. J., Shenbaga Velu P., Simulation of Friction Welding of Alumina and Steel with Aluminium Interlayer,** International Journal of Advanced Manufacturing Technology, Vol. 93, 2017, pp. 121-127, <https://doi.org/10.1007/s00170-015-7874-8>.
- [80] **Kundu S., Chatterjee S., Characterisation of Diffusion Bonded Joint between Titanium and 304 Stainless Steel Using a Ni Interlayer,** Materials Characterization, Vol. 59, 2008, pp. 631-637, <https://doi.org/10.1016/j.matchar.2007.05.015>.
- [81] **Wang X., Li W., Ma T., Yang X., Vairis A., Effect of Welding Parameters on the Microstructure and Mechanical Properties of Linear Friction Welded Ti-6.5Al-3.5Mo-1.5Zr-0.3Si Joints,** Journal of Manufacturing Process, Vol. 46, 2019, pp. 100-108, <https://doi.org/10.1016/j.jmapro.2019.08.031>.
- [82] **Kuznetsov M. A., Zernin E. A., Nanotechnologies and nanomaterials in welding production (review),** Welding International, Vol. 26(4), 2012, pp. 311-313, <https://doi.org/10.1080/09507116.2011.606158>.
- [83] **Rotundo F., Marconi A., Morri A., Ceschini A., Dissimilar Linear Friction Welding Between a Sic Particle Reinforced Aluminium Composite and a Monolithic Aluminium Alloy: Microstructural, Tensile and Fatigue Properties,** Materials Science & Engineering A, Vol. 559, 2013, pp. 852-860. <https://doi.org/10.1016/j.msea.2012.09.033>.
- [84] **Li P., Li J., Dong H., Ji C., Metallurgical and Mechanical Properties of Continuous Drive Friction Welded Copper/Alumina Dissimilar Joints,** Materials & Design, Vol. 127, 2017, pp. 311-319. <https://doi.org/10.1016/j.matdes.2017.04.093>.
- [85] **Wincizenko R., Goroch O., Krzynska A., Kaczorowski M., Friction Welding of Tungsten Heavy Alloy with Aluminium Alloy,** Journal of Materials Processing Technology, Vol. 246, 2017, pp. 42-55, <http://dx.doi.org/10.1016/j.jmatprotech.2017.03.009>.
- [86] **Tra H T., Sakaguchi M., High Cycle Fatigue Behaviour of the IN718/M247 Hybrid Element Fabricated by Friction Welding at Elevated Temperatures,** Journal of Science: Advanced Materials and Devices, Vol. 1, 2016, pp. 501-506, <http://dx.doi.org/10.1016/j.jsamd.2016.08.009>.
- [87] **Li P., Dong H., Xia Y., Hao X., Shuai W., Pan L., Jun Z., Inhomogeneous Interface Structure and Mechanical Properties of Rotary Friction Welded TC4 Titanium Alloy/316L Stainless Steel Joints,** Journal of Manufacturing Processes, Vol. 33, 2018, pp. 54-63, <https://doi.org/10.1016/j.jmapro.2018.05.001>.
- [88] **Pandiarajan S., Senthil Kumaran S., Kumaraswamidhas L.A., Saravanan R., Interfacial Microstructure and Optimization of Friction Welding by Taguchi and ANOVA on SA 213 Tube to SA 387 Tube Plate without Backing Block using an External Tool,** Journal of Alloys and Compounds, Vol. 654, 2016, pp. 534-545, <http://dx.doi.org/10.1016/j.jallcom.2015.09.152>.
- [89] **Hynes R. J., Velu P. S., Effect of Rotational Speed on Ti-6Al-4V-AA 6061 Friction Welded Joints,** Journal of Manufacturing Processes, Vol. 32, 2018, pp. 288-297, <https://doi.org/10.1016/j.jmapro.2018.02.014>.
- [90] **Isik E., Özes C., Determination of the Mechanical Properties of Friction Welded Tube Yoke and Tube Joint,** Advances in Materials Science and Engineering, Vol. 2016, 8918253, 2016, <http://dx.doi.org/10.1155/2016/8918253>.
- [91] **Hangai Y., Nakano Y., Koyama S., Kuwazuru O., Kitahara S., Yoshikawa N., Fabrication of Aluminum Tubes Filled with Aluminum Alloy Foam by Friction Welding,** Materials, Vol. 8, 2015, pp. 7180-7190, <https://doi.org/10.3390/ma8105373>.
- [92] **Senthil Kumaran S., Srinivasan K., Narayanan S., Joseph Raj A. N., Prediction of Tensile Strength in Friction Welding Joints Made of SA213 Tube to SA387 Tube Plate through Optimization Techniques,** Materials, Vol. 12, 4079, 2019, <https://doi.org/10.3390/ma12244079>.
- [93] **Ji Y., Wu S., Zhao D., Microstructure and Mechanical Properties of Friction Welding Joints with Dissimilar Titanium Alloys,** Metals, Vol. 6, 108, 2016, <https://doi.org/10.3390/met605108>.
- [94] **Rossi S., Russo F., Lemmi A. M., Benedetti M., Fontanar V., Fatigue Corrosion Behavior of Friction Welded Dissimilar Joints in Different Testing Conditions,** Metals, Vol. 10, 1018, 2020, [doi:10.3390/met10081018](https://doi.org/10.3390/met10081018).
- [95] **Packiaraj Rajendran T., Hynes N. R. J., Christopher T., Characterization of High-Carbon High-Chromium Tool Steel/Low-Carbon Steel Friction-Welded Joints for Industrial Tooling Applications,** Journal of the Brazilian Society of Mechanical Sciences and Engineering, Vol. 40(316), 2018, <https://doi.org/10.1007/s40430-018-1243-0>.
- [96] **Hynes N. R. J., Nagaraj P., Basil S. J., Numerical Simulation on Joining of Ceramics with Metal by Friction Welding Technique,** International Journal of Modern Physics: Conference Series, Vol. 22, 2013, pp. 190-195, <https://doi.org/10.1142/S2010194513010118>.
- [97] **Liu Y., Zhao H., Peng Y., Ma X., Mechanical Properties of the Inertia Friction Welded Aluminum/Stainless Steel Joint,** Welding

- in the World, Vol. 63, 2019, pp. 1601-1611, <https://doi.org/10.1007/s40194-019-00793-2>.
- [98] **Cheepu M., Ashfaq M., Muthupandi V.,** *A New Approach for using Interlayer and Analysis of the Friction Welding of Titanium to Stainless Steel*, Transactions of the Indian Institute of Metals, Vol. 70(10), 2017, pp. 2591-2600, <http://dx.doi.org/10.1007/s12666-017-1114-x>.
- [99] **Kannan P., Balamurugan K., Thirunavukkarasu K.,** *An Experimental Study on The Effect of Silver Interlayer on Dissimilar Friction Welds 6061-T6 Aluminium MMC And AISI 304 Stainless Steel*, Indian Journal of Engineering and Materials Science, Vol. 21, 2014, pp. 635-646, <http://hdl.handle.net/123456789/30523>.
- [100] **Sinha H., Corneliusson J., Turba K., Iyengar S.,** *A Study on the Formation of Iron Aluminide (FeAl) from Elemental Powders*, Journal of Alloys and Compounds, Vol. 636, 2015, pp. 261-269, <http://dx.doi.org/10.1016/j.jallcom.2015.02.132>.
- [101] **Murray J. L.,** *Fe-Al Binary Phase Diagram, Alloy Phase Diagrams (Book)*, ASM International, Materials Park, USA, 1992, pp. 54.
- [102] **Li X., Scherf A., Heilmaier M., Stein F.,** *The Al-Rich Part of the Fe-Al Phase Diagram*, Journal of Phase Equilibria and Diffusion, Vol. 37, 2016, pp. 162-173, [10.1007/s11669-015-0446-7](https://doi.org/10.1007/s11669-015-0446-7).
- [103] **Satpathy M. P., Patel B., Kumar Sahoo S.,** *Exploration of Bonding Phenomenon and Microstructural Characterisation During High-Power Ultrasonic Spot Welding of Aluminium to Steel Sheets with Copper Interlayer*, Ain Shams Engineering Journal, Vol. 10(4), 2019, pp. 811-819, <http://doi.org/10.1016/j.asej.2019.07.007>.
- [104] **Vyas H., Mehta K. P., Badheka V., Doshi B.,** *Pipe-To-Pipe Friction Welding of Dissimilar Al-SS Joints for Cryogenic Applications*, Journal of the Brazilian Society of Mechanical Sciences and Engineering, Vol. 42(96), 2020, pp. 1-12, <https://doi.org/10.1007/s40430-020-2181-1>.
- [105] **Karthik G. M., Mastanaiah P., Janaki Ram G. D., Kottada R. S.,** *Friction Buttering: A New Technique for Dissimilar Welding*, Metallurgical and Materials Transactions B, Vol. 48(3), 2017, pp. 1416-1422, [10.1007/s11663-017-0934-8](https://doi.org/10.1007/s11663-017-0934-8).
- [106] **Mahto R. P., Kumar R., Pal S. K., Panda S. K.,** *A Comprehensive Study on Force, Temperature, Mechanical Properties and Micro-Structural Characterizations in Friction Stir Lap Welding of Dissimilar Materials (AA6061-T6 & AISI304)*, Journal of Manufacturing Processes, Vol. 31, 2018, pp. 624-639, <https://doi.org/10.1016/j.jmapro.2017.12.07>.
- [107] **Reddi Prasad K., Sridhar V. G.,** *Evaluating the Capability, Joining and Characterization of Similar and Dissimilar Pipes by Friction Welding Process-Review*, International Journal of Applied Engineering Research, Vol. 11(5), 2016, pp. 3681-3688.
- [108] **Shubhavardhan R. N., Surendran S.,** *Friction Welding To Joint Stainless Steel and Aluminium Materials*, International Journal of Metallurgical and Materials Science and Engineering, Vol. 2(3), 2012, pp. 53-73.
- [109] **Alves E. P., An C. Y., Neto F. P., Ferro Dos Santos E.,** *Experimental Determination of Temperature During Rotary Friction Welding of Dissimilar Materials*, Frontiers in Aerospace Engineering, Vol. 1(1), 2012, pp. 20-26.
- [110] **Dong H., Li Y., Li P., Hao X., Xia Y., Yang G.,** *Inhomogeneous microstructure and mechanical properties of rotary friction welded joints between 5052 aluminum alloy and 304 stainless steel*, Journal of Materials Processing Technology, Vol. 272, 2019, pp. 17-27, <https://doi.org/10.1016/j.jmatprotec.2019.04.039>.
- [111] **Celik S., Karaoglan A. D., Ersozlu I.,** *An Effective Approach Based on Response Surface Methodology for Predicting Friction Welding Parameters*, High Temperature Materials and Processes, Vol. 35(3), 2016, pp. 235-241, [10.1515/htmp-2014-0201](https://doi.org/10.1515/htmp-2014-0201).
- [112] **Pilli N., Senapati A. K., Moora S. L.,** *Review on Process Parameters of Similar and Dissimilar Materials in Friction Welding*, AIP Conference Proceedings, 2327, 020049, 2021, <https://doi.org/10.1063/5.0039834>.
- [113] **Li P., Li J., Dong H.,** *Analytical Description of Heat Generation and Temperature Field During the Initial Stage of Rotary Friction Welding*, Journal of Manufacturing Process, Vol. 25, 2017, pp. 181-184, <https://doi.org/10.1016/j.jmapro.2016.12.003>.
- [114] **Ratkovic N., Arsic D., Lazic V., Nikolic R. R., Hadzima B.,** *Microstructure in the Joint Friction Plane in Friction Welding of Dissimilar Steels*, Procedia Engineering, Vol. 149, 2016, pp. 414-420, <https://doi.org/10.1016/j.proeng.2016.06.686>.
- [115] **Mercen S., Aydin S., Ozzdemir N.,** *Effect of Welding Parameters on the Fatigue Properties of Dissimilar AISI 2205-AISI 1020 Joined by Friction Welding*, International Journal of Fatigue, Vol. 81, 2015, pp. 78-90, <https://doi.org/10.1016/j.ijfatigue.2015.07.023>.
- [116] **Ochi H., Ogawa K., Yamamoto Y., Suga Y.,** *Friction Welding of Aluminium Alloy and Steel*, International Journal of Offshore and Polar Engineering, Vol. 8(2), ISOPE-98-08-2-140, 1998.
- [117] **Leitao C., Arruti E., Aldanondo E., Rodrigues D. M.,** *Aluminium-Steel Lap Joining by Multi Pass Friction Stir Welding*, Materials and Design, Vol. 106, 2016, pp. 153-160, <https://doi.org/10.1016/j.matdes.2016.05.101>.
- [118] **Ajith P. M., Afsal Husain T. M., Sathiya P., Aravindan S.,** *Multi-Objective Optimisation of Continuous Drive Friction Welding Process Parameters using Response Surface Methodology with Intelligent Optimization Algorithm*, Journal of Iron and Steel Research International, Vol. 22(10), 2015, pp. 954-960, [https://doi.org/10.1016/S1006-706X\(15\)30096-0](https://doi.org/10.1016/S1006-706X(15)30096-0).
- [119] **Singh R., Kumar R., Feo L., Fraternali F.,** *Friction Welding of Dissimilar Plastic/Polymer Materials with Metal Powder Reinforcement for Engineering Applications*, Composites Part B, Vol. 101, 2016, pp. 77-86, <https://doi.org/10.1016/j.compositesb.2016.06.082>.
- [120] **Paventhana R., Lakshminarayan P. R., Balasubramanian V.,** *Prediction and Optimisation of Friction Welding Parameters for Joining Aluminium Alloy and Stainless Steel*, Transactions of Nonferrous Metals Society of China, Vol. 21, 2011, pp. 1480-1485, [https://doi.org/10.1016/S1003-6326\(11\)60884-4](https://doi.org/10.1016/S1003-6326(11)60884-4).
- [121] **Bennett C.,** *Finite element modelling of the inertia friction welding of a CrMoV alloy steel including the effects of solid-state phase transformations*, Journal of Manufacturing Processes, Vol. 18, 2015, pp. 84 - 91, <https://doi.org/10.1016/j.jmapro.2015.01.003>.
- [122] **Song Changbao, Lin Tiesong, He Peng, Jiao Zhen, Tao Jun, and Ji Yajuan.,** *Molecular Dynamics Simulation of Linear Friction Welding Between Dissimilar Ti-Based Alloy*, Computational Materials Science, Vol. 83, 2014, pp. 35-38, <https://doi.org/10.1016/j.commatsci.2013.11.013>.
- [123] **Lis A., Mogami H., Matsuda T., Sano T., Yoshida R., Hori H., Hirose A.,** *Hardening and Softening Effects in Aluminium Alloys During High-Frequency Linear Friction Welding*, Journal of Materials Processing Technology, Vol. 255, 2018, pp. 547-558, <https://doi.org/10.1016/j.jmatprotec.2018.01.002>.
- [124] **Palanivel R., Laubscher R.F., Dinaharan I.,** *An Investigation into the Effect of Friction Welding Parameters on Tensile Strength of Titanium Tubes by Utilizing an Empirical Relationship*, Measurement, Vol. 98, 2017, pp. 77-91, <http://dx.doi.org/10.1016/j.measurement.2016.11.035>.
- [125] **Raji Reddy D., Laxminarayana P., Reddy G. C. M., Reddy G. M. S.,** *Process Parameters Influence on Impact Toughness and Microstructure of Pre-Heat Treated Friction Welded 15CDV6 Alloy Steel*, International Journal of Engineering and Manufacturing, Vol. 5, 2016, pp. 38-47, [10.5815/ijem.2016.05.05](https://doi.org/10.5815/ijem.2016.05.05).
- [126] **Romero J., Attallah M. M., Preuss M., Karadge M., Bray S. E.,** *Effect of the Forging Pressure on the Microstructure and Residual Stress Development in Ti-6Al-4V Linear Friction Welds*, Acta Materialia, Vol. 57, 2009, pp. 5582-5592, [10.1016/j.actamat.2009.07.055](https://doi.org/10.1016/j.actamat.2009.07.055).
- [127] **Zhou Y., Zhang J., North T. H., Wang Z.,** *The Mechanical Properties of Friction Welded Aluminium-Based Metal-Matrix Composite Materials*, Journal of Materials Science, Vol. 32, 1997, pp. 3883-3889, <https://doi.org/10.1023/A:1018652429477>.
- [128] **Deepak M., Ananthapadmanaban D.,** *Welding Mechanisms During Friction Welding of Aluminium with Steel*, Journal of Chemical and Pharmaceutical Sciences, Special Issue 7, SPB Pharma Society, 2017.
- [129] **Palanivel R., Laubscher R. F., Dinaharan I., Hattingh D.G.,** *Microstructure and Mechanical Characterisation of Continuous Drive Friction Welded Grade 2 Seamless Titanium Tubes at Different Rotational Speeds*, International Journal of Pressure Vessels and Piping, Vol. 154, 2017, pp. 17-28, <http://dx.doi.org/10.1016/j.ijpvp.2017.06.005>.
- [130] **Sreenivasan K. S., Satish Kumar S., Katiravan J.,** *Genetic Algorithm Based Optimization of Friction Welding Process*

*Parameters on AA7075-Sic Composite*, Engineering Science and Technology, an International Journal, Vol. 22, 2019, pp. 1136-114. <https://doi.org/10.1016/j.jestch.2019.02.010>.

[131] **Chludzinski M., Dos Santos R. E., Ramming Pissanti D., Cantelli Kroeff F., Matteib F., Dalpiaz G., Torres Piza Paes M.**, *Full-scale friction welding system for pipeline Steels*, Journal of Materials Research and Technology, Vol. 8(2), 2019, pp. 1773-1780. <https://doi.org/10.1016/j.jmrt.2018.12.007>.

[132] **Barua D., Welo T., Ringen G., Wang J.**, *An Experimental Study on Interference Friction Welding Process*, Procedia Manufacturing, Vol. 41, 2019, pp. 1149-1155. [10.1016/j.promfg.2019.12.001](https://doi.org/10.1016/j.promfg.2019.12.001).

[133] **Liu W., Wang F., Yang X., Li W.**, *Upset Prediction in Friction Welding Using Radial Basis Function Neural Network*. *Advances in Materials Science and Engineering*, Vol. 2013, 196382, 2013, <http://dx.doi.org/10.1155/2013/196382>.

[134] **Wang G., Li J., Wang W., Xiong J. Zhang F.**, *Study on the Effect of Energy-Input on the Joint Mechanical Properties of Rotary Friction Welding*, Metals, Vol. 8, 908, 2018, [10.3390/met8110908](https://doi.org/10.3390/met8110908).

[135] **Lai F., Qu S., Lewis R., Slatter T., Sun G., Zhang T., Xiaoqiang L.**, *Optimization of Friction Welding Process Parameters for 42Cr9Si2 Hollow Head and Sodium Filled Engine Valve and Valve Performance Evaluation*, Materials, Vol. 12, 1123, 2019, [doi:10.3390/ma12071123](https://doi.org/10.3390/ma12071123).

[136] **Senthil Murugan S., Noorul Haq A., Sathiya P.**, *Eco-Friendly Frictional Joining of AA6063 and AISI304L Dissimilar Metals and Characterisation of Bimetal Joints*, Journal of New Materials for Electrochemical Systems, Vol. 23(2), PP-101-111, 2020, <https://doi.org/10.14447/jnmes.v23i2.a07>.

[137] **Senthil Murugan S., Sathiya P., Noorul Haq A.**, *Experimental Study on the Effect of Silver, Nickel and Chromium Interlayers and Upset Pressure in Joining SS304L-AA6063 Alloys through Direct Drive Friction Welding Process*, Journal of the Brazilian Society of Mechanical Sciences and Engineering, Vol. 42(611), 2020, pp. 1-17. <https://doi.org/10.1007/s40430-020-02687-7>.

[138] **Senthil Murugan S., Sathiya P., Noorul Haq A.**, *Continuous Drive Dissimilar Friction Welding of Wrought Aluminium-6063-T6 and Austenitic Stainless Steel-304L with Different Faying Surfaces and Welding Trials*, Kovové Materiály - Metallic Materials. Vol. 59(3), 2021, pp. 161-179, [10.4149/km.20213161](https://doi.org/10.4149/km.20213161).

[139] **Senthil Murugan S., Sathiya P., Noorul H. A. H.**, *Effect of faying surfaces and characterization of aluminium AA6063-steel AISI304L Dissimilar joints fabricated by friction welding with Hemispherical Bowl, and Threaded Faying Surfaces*, The International Journal of Advanced Manufacturing Technology, Vol. 116, 2021, pp. 629-666, [10.1007/s00170-021-07445-0](https://doi.org/10.1007/s00170-021-07445-0).